BOSTON UNIVERSITY

c Flow Around Complex

. Chen, E.O. Suciu and

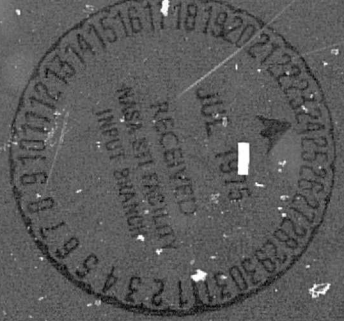

DEPARTMENT OF AEROSPACE ENGINEERING

COLLEGE OF ENGINEERING

BOSTON, MASSACHUSETTS

DEPARTMENT OF AEROSPACE ENGINEERING
BOSTON UNIVERSITY
COLLEGE OF ENGINEERING
BOSTON, MASS 02215

A FINITE-ELEMENT ANALYSIS FOR STEADY AND OSCILLATORY SUBSONIC FLOW AROUND COMPLEX CONFIGURATIONS

L.T. Chen, E.O. Suciu
and
L. Morino

December 1974

Prepared for

LANGLEY RESEARCH CENTER
NATIONAL AERONAUTICS AND SPACE ADMINISTRATION
HAMPTON, VIRGINIA 23365

Under

NASA Grant NGR 22-004-030
E. Carson Yates, Jr., Technical Advisor

ABSTRACT

The problem of potential subsonic flow around complex configurations is considered. This problem requires the solution of an integral equation relating the values of the potential on the surface of the body to the values of the normal derivative, which is known from the boundary conditions. The surface of the body is divided into small (hyperboloidal quadrilateral) surface elements, Σ_ℓ, which are described in terms of the Cartesian components of the four corner points. The values of the potential (and its normal derivative) within each element is assumed to be constant and equal to its value at the centroid of the element. This yields a set of linear algebraic equations. The coefficients of the equation are given by source and doublet integrals over the surface elements, Σ_ℓ. Closed form evaluations of the integrals are presented. The results obtained with the above formulation are compared with existing analytical and experimental results.

FOREWORD

This research is supported by a NASA Grant NGR 22-004-030. Dr. E. Carson Yates, Jr. of NASA Langley Research Center acted as technical advisor. The authors wish to express their appreciation to Dr. Yates for the stimulating discussions and invaluable suggestions made in connection with this work.

TABLE OF CONTENTS

TABLE OF CONTENTS, Continued

LIST OF ILLUSTRATIONS

LIST OF ILLUSTRATIONS (Continued)

LIST OF SYMBOLS

$\vec{a}_i$	base vectors, Eqs. 1.13 and 2.8
b_h	see Eq. 1.9
b_{hk}	see Eq. 1.10
c_p	pressure coefficient
$c_\ell = -\Delta c_p = c_{p,\ell} - c_{p,u}$	lifting pressure coefficient
c_{ki}	see Eq. 1.8
$I_D(\xi, \eta)$	see Eqs. 2.16
$I_S(\xi, \eta)$	see Eqs. 2.17
$J_W(\xi, \eta)$	see Eqs. 3.12 and 3.13
$\vec{n}$	normal to the surface Σ at P_1
N	number of elements
$P \equiv (X,Y,Z)$	control point
P_{++}, P_{+-}, P_{-+}, P_{--}	see Eq. 2.4
P_c, P_1, P_2, P_3	see Eq. 2.2
P_0	see Eq. 2.11
$P^{(k)}$	centroid of element
$\vec{q}$	see Eq. 2.10

$$r = \left[(x - x_1)^2 + (y - y_1)^2 + (z - z_1)^2\right]^{1/2}$$

r_h	see Eq. 2.10
U_∞	velocity of undisturbed flow
w_{ki}	see Eqs. 3.4 and 3.5
x,y,z	Cartesian coordinates
γ	vorticity
δ_{ki}	Kronecker delta
ξ, η	see Eq. 2.7
ρ_∞	density of undisturbed air
σ	surface surrounding body and wake
σ_K	surface element
φ	perturbation aerodynamic potential
φ_K	value of φ at $P^{(k)}$
Φ	aerodynamic potential
Ω	solid angle

SPECIAL SYMBOLS

∇	gradient operator in x,y,z coordinates

SUBSCRIPTS

1	Dummy variables
TE	trailing edge
*	evaluation at $P = P_*$

SECTION I

FORMULATION OF THE PROBLEM

1.1 Introduction

A general theory for compressible unsteady potential aerodynamic flow around lifting bodies having arbitrary shapes and motions is given in Refs. 1 and 2. Application to finite-thickness steady and oscillating wings in subsonic flow is given in Refs. 3, 4, and 5. A general numerical formulation for complex configurations in subsonic flow is considered in Ref. 6. Applications of this formulation are considered here. For simplicity, only the incompressible flow is considered in detail*. In this case, the problem is governed by the Laplace equation with prescribed normal derivative on the body (exterior Neumann problem for the Laplace equation) with an additional complication due to the presence of the wake (of unknown geometry).

The problem of the evaluation of the steady, incompressible potential aerodynamic flow around an aircraft of arbitrary configuration can be analyzed by solving the integral equation

$$\varphi_* = -\frac{1}{2\pi} \oint_{\sigma} \left[\frac{\partial \varphi}{\partial n} \frac{1}{r} - \varphi \frac{\partial}{\partial n} \left(\frac{1}{r} \right) \right] d\sigma \qquad (1.1)$$

where σ is a surface surrounding the aircraft and the wake[2,5] (Fig. 1). For the moment, it will be assumed that the wake does not exist. The effect of the wake is considered in Section III.

---

* Subsonic oscillatory flow is considered in Appendix A.

The value of $\frac{\partial \varphi}{\partial n}$ is obtained from the boundary condition (tangency condition)

$$\frac{\partial \phi}{\partial r} = U_\infty \frac{\partial}{\partial n}(x + \varphi) = U_\infty \left(n_x + \frac{\partial \varphi}{\partial n}\right) = 0 \tag{1.2}$$

or

$$\frac{\partial \varphi}{\partial n} = -n_x = -\bar{n} \cdot \bar{i} \tag{1.3}$$

The integral equation can be studied by dividing the surface σ into N small finite elements σ_i (see Fig. 2) to yield

$$\varphi_* = \frac{1}{2\pi} \sum_{k=1}^{N} \iint_{\sigma_k} \left[\bar{n} \cdot \bar{i} \, \frac{1}{r} + \varphi \, \bar{n} \cdot \bar{\nabla}\left(\frac{1}{r}\right) \right] d\sigma_k \tag{1.4}$$

Applying the mean value theorem one obtains

$$\varphi_* = \frac{1}{2\pi} \sum_{k=1}^{N} \iint_{\sigma_k} \left(\bar{n} \cdot \bar{i} \, \frac{1}{r} \right) d\sigma_k + \frac{1}{2\pi} \sum_{k=1}^{N} \varphi_k \iint_{\sigma_k} \bar{n} \cdot \bar{\nabla}\left(\frac{1}{r}\right) d\sigma_k \tag{1.5}$$

where φ_k is a suitable mean value of φ inside the element σ_k, which will be approximated by the value of φ at the centroid $p^{(k)}$ of the element, σ_k .

By satisfying Eq. (1.5) at the centroid, $p^{(h)}$, of the element σ_h , (h = 1, 2...N) yields

$$\varphi_h = \frac{1}{2\pi} \sum_{k=1}^{N} \bar{n}_k \cdot \bar{i} \iint_{\sigma_k} \frac{1}{r_h} \, d\sigma_k +$$

$$\frac{1}{2\pi} \sum_{k=1}^{N} \varphi_k \iint_{\sigma_k} \bar{n} \cdot \bar{\nabla}\left(\frac{1}{r_h}\right) d\sigma_k \qquad (h = 1, 2, 3, \ldots N) \tag{1.6}$$

where r_h is the distance of the centroid of the element σ_h from the dummy point of integration in the element σ_k .

Equation (1.6) is equivalent to*

$$\left[\delta_{hk} - C_{hk} \right] \{ \varphi_k \} = \{ b_h \} \tag{1.7}$$

where

$$C_{hk} = \frac{1}{2\pi} \iint_{\sigma_k} \bar{n} \cdot \bar{v} \frac{1}{r_h} \, d\sigma_k \tag{1.8}$$

and

$$\{ b_h \} = [b_{hk}] \{ \bar{n}_k \cdot \bar{i} \} \tag{1.9}$$

with

$$b_{hk} = \frac{1}{2\pi} \iint_{\sigma_k} \frac{1}{r_h} \, d\sigma_k \tag{1.10}$$

1.2 Surface Geometry

Let the geometry of the element σ_K be described by

$$\vec{P} = \vec{P}(\xi^1, \xi^2) \tag{1.11}$$

where ξ^1 and ξ^2 are the generalized curvilinear coordinate. Then the two base vectors $\vec{a}_i$ are given by (Fig. 3)

$$\vec{a}_i = \frac{\partial \vec{P}}{\partial \xi^i} \tag{1.12}$$

The unit normal to the surface is given by

$$\vec{n} = \frac{\vec{a}_1 \times \vec{a}_2}{| \vec{a}_1 \times \vec{a}_2 |} \tag{1.13}$$

---

*The effect of the wake is not considered here (see Section III).

and is directed according to the right-hand rule (Fig. 3.).
The surface element $d\sigma$ is given by (Fig. 3)

$$d\sigma = \left| \vec{a}_1 d\xi^1 \times \vec{a}_2 d\xi^2 \right| = \left| \vec{a}_1 \times \vec{a}_2 \right| d\xi^1 d\xi^2 \tag{1.14}$$

1.3 Expressions for b_{hk} and c_{hk}

Combining Eqs. (1.10), (1.13) and (1.14) yields

$$b_{hk} = \frac{1}{2\pi} \iint_{\sigma_k} \frac{|\bar{a}_1 \times \bar{a}_2|}{r} d\xi^1 d\xi^2 \tag{1.15}$$

Similarly, combining Eqs. (1.8), (1.13) and (1.14) yields

$$\begin{aligned} c_{hk} &= \frac{1}{2\pi} \iint_{\sigma_k} \bar{a}_1 \times \bar{a}_2 \cdot \bar{\nabla} \left(\frac{1}{r} \right) d\xi^1 d\xi^2 \\ &= -\frac{1}{2\pi} \iint_{\sigma_k} \frac{\bar{a}_1 \times \bar{a}_2 \cdot \bar{q}}{r^3} d\xi^1 d\xi^2 \end{aligned} \tag{1.16}$$

where

$$\bar{q} = \begin{Bmatrix} x - x_h \\ y - y_h \\ z - z_h \end{Bmatrix} \tag{1.17}$$

and

$$r = |\bar{q}| \tag{1.18}$$

SECTION II

HYPERBOLOIDAL ELEMENT

2.1 Introduction

Consider the equations

$$\begin{aligned} x &= x_c + x_1\xi + x_2\eta + x_3\xi\eta \\ y &= y_c + y_1\xi + y_2\eta + y_3\xi\eta \\ z &= z_c + z_1\xi + z_2\eta + z_3\xi\eta \end{aligned} \tag{2.1}$$

or, in vector notations

$$\bar{P} = \bar{P}_c + \bar{P}_1\xi + \bar{P}_2\eta + \bar{P}_3\xi\eta \tag{2.2}$$

This represents a hyperboloid. The lines η = const and ξ = const are clearly straight lines. Consider the hyperboloidal element defined by the above equation with

$$\begin{aligned} -1 \le \xi \le 1 \\ -1 \le \eta \le 1 \end{aligned} \tag{2.3}$$

The centroid of the element is $\bar{P}_c$ ($\xi = \eta = 0$). The corner points of this element are

$$\begin{aligned} \bar{P}_{++} &= \bar{P}_c + \bar{P}_1 + \bar{P}_2 + \bar{P}_3 && (\xi = +1,\ \eta = +1) \\ \bar{P}_{+-} &= \bar{P}_c + \bar{P}_1 - \bar{P}_2 - \bar{P}_3 && (\xi = +1,\ \eta = -1) \\ \bar{P}_{-+} &= \bar{P}_c - \bar{P}_1 + \bar{P}_2 - \bar{P}_3 && (\xi = -1,\ \eta = +1) \\ \bar{P}_{--} &= \bar{P}_c - \bar{P}_1 - \bar{P}_2 + \bar{P}_3 && (\xi = -1,\ \eta = -1) \end{aligned} \tag{2.4}$$

The inverse relation is

$$\bar{P}_0 = \frac{1}{4}(\bar{P}_{++} + \bar{P}_{+-} + \bar{P}_{-+} + \bar{P}_{--})$$

$$\bar{P}_1 = \frac{1}{4}(\bar{P}_{++} + \bar{P}_{+-} - \bar{P}_{-+} - \bar{P}_{--})$$

$$\bar{P}_2 = \frac{1}{4}(\bar{P}_{++} - \bar{P}_{+-} + \bar{P}_{-+} - \bar{P}_{--})$$

$$\bar{P}_3 = \frac{1}{4}(\bar{P}_{++} - \bar{P}_{+-} - \bar{P}_{-+} + \bar{P}_{--}) \qquad (2.5)$$

Note that the four boundaries of the element ($\xi = \pm 1$, $\eta = \pm 1$) are straight lines given by

$$\bar{P} = (\bar{P}_0 + \bar{P}_1) + (\bar{P}_2 + \bar{P}_3)\eta \qquad -1 \le \eta \le 1$$

$$\bar{P} = (\bar{P}_0 - \bar{P}_1) + (\bar{P}_2 - \bar{P}_3)\eta \qquad -1 \le \eta \le 1$$

$$\bar{P} = (\bar{P}_0 + \bar{P}_2) + (\bar{P}_1 + \bar{P}_3)\xi \qquad -1 \le \xi \le 1$$

$$\bar{P} = (\bar{P}_0 - \bar{P}_2) + (\bar{P}_1 - \bar{P}_3)\xi \qquad -1 \le \xi \le 1 \qquad (2.6)$$

Next, assume that the surface of the aircraft is divided into curved quadrilateral elements with four corner points $\bar{P}_{++}$, $\bar{P}_{+-}$, $\bar{P}_{-+}$, $\bar{P}_{--}$. Then, as mentioned in Section I, these elements can be replaced by the hyperboloidal element (described above) which goes through the four corner points $\bar{P}_{++}$, $\bar{P}_{+-}$, $\bar{P}_{-+}$, $\bar{P}_{--}$ (see Fig. 4). It may be noted that the surface is continuous since adjacent elements have in common the straight line connecting the two common corner points. It

may be noted also the $\bar{P}_c$ is the centroid of the hyperboloidal element G_k and hence it will be indicated as

$$\bar{P}_c = \bar{P}^{(k)} \tag{2.6}$$

2.2 Geometry of Hyperboloid Element

The geometric quantities introduced in Section I can be written for the hyperboloid element described above. Letting

$$\xi^1 = \xi \quad , \qquad \xi^2 = \eta \tag{2.7}$$

Equation (1.12) yields

$$\bar{a}_1 = \frac{\partial \bar{P}}{\partial \xi} = \bar{P}_1 + \bar{P}_3 \eta \tag{2.8-a}$$

$$\bar{a}_2 = \frac{\partial \bar{P}}{\partial \eta} = \bar{P}_2 + \bar{P}_3 \xi \tag{2.8-b}$$

This yields

$$\bar{a}_1 \times \bar{a}_2 = (\bar{P}_1 \times \bar{P}_3 \eta) \times (\bar{P}_2 \times \bar{P}_3 \xi) =$$

$$\bar{P}_1 \times \bar{P}_2 + \bar{P}_1 \times \bar{P}_3 \xi + \bar{P}_3 \times \bar{P}_2 \eta \tag{2.9}$$

since $\bar{P}_3 \times \bar{P}_3 = 0$.

Note that, with present notations

$$\bar{q} = \bar{r}_h = \bar{P} - \bar{P}^{(h)} = \bar{P}^{(k)} - \bar{P}^{(h)} + \bar{P}_1 \xi + \bar{P}_2 \eta + \bar{P}_3 \xi \eta =$$

$$\bar{P}_0 + \bar{P}_1 \xi + \bar{P}_2 \eta + \bar{P}_3 \xi \eta \tag{2.10}$$

where

$$\bar{P}_0 = \bar{P}^{(k)} - \bar{P}^{(h)} \tag{2.11}$$

is the vector connecting the centroid $\bar{P}^{(h)}$ of the element σ_h, to the one, $\bar{P}^{(k)}$, of the element σ_k.

2.3 Expressions for b_{hk} and c_{hk}

Introducing the functions I_S and I_D (indefinite source and doublet integrals) such that

$$\frac{\partial^2 I_S}{\partial \xi \partial \eta} = \frac{1}{2\pi} \frac{|\bar{a}_1 \times \bar{a}_2|}{r} \tag{2.12}$$

and

$$\frac{\partial^2 I_D}{\partial \xi \partial \eta} = -\frac{1}{2\pi} \frac{\bar{a}_1 \times \bar{a}_2 \cdot \bar{q}}{r^3} \tag{2.13}$$

Equations (1.15) and (1.16) may be rewritten as

$$b_{hk} = I_S(1,1) - I_S(1,-1) - I_S(-1,1) + I_S(-1,-1) \tag{2.14}$$

$$c_{hk} = I_D(1,1) - I_D(1,-1) - I_D(-1,1) + I_D(-1,-1) \tag{2.15}$$

In Ref. 6, the expressions for I_S and I_D have been obtained as (the proof is included here in Appendix B).

$$I_D(\xi,\eta) = \frac{1}{2\pi} \tan_\rho^{-1}\left(\frac{\bar{q}\times\bar{a}_1 \cdot \bar{q}\times\bar{a}_2}{|\bar{q}|\,\bar{q}\cdot\bar{a}_1\times\bar{a}_2}\right) \tag{2.16}$$

$$I_S(\xi,\eta) = -\frac{1}{2\pi}\left\{-\bar{q}\times\bar{a}_1\cdot\bar{n}\,\frac{1}{|\bar{a}_1|}\,\ln\left||\bar{q}||\bar{a}_1| + \bar{q}\cdot\bar{a}_1\right| + \bar{q}\times\bar{a}_2\cdot\bar{n}\,\frac{1}{|\bar{a}_2|}\ln\left||\bar{q}||\bar{a}_2| + \bar{q}\cdot\bar{a}_2\right| + \bar{q}\cdot\bar{n}\,\tan_\rho^{-1}\left(\frac{\bar{q}\times\bar{a}_1\cdot\bar{q}\times\bar{a}_2}{|\bar{q}|\,\bar{q}\cdot\bar{a}_1\times\bar{a}_2}\right)\right\} \tag{2.17}$$

2.4 Solution of Problem

The wake contribution is shown in detail in Section III. Equation 1.7 can now be solved for φ_k, (see also Ref. 7 . The linearized Bernoulli Theorem will further give the pressure distribution:

$$c_p = -2 \frac{\partial \varphi}{\partial x} \tag{2.18}$$

2.5 Wing and Body Geometry

This subsection presents the geometry of the wings and wing-body combinations which were used for obtaining the results presented in Section IV.

2.5.1 Wing Geometry

First, the wing geometry is presented. The projection of the wing on the xy plane is given by

$$\begin{aligned} \bar{X}_{L.E.} &= \bar{X}_{L.E.}(\bar{y}) \\ \bar{X}_{T.E.} &= \bar{X}_{T.E.}(\bar{y}) \end{aligned} \tag{2.19}$$

where L.E. and T.E. stand for leading edge and trailing edge, respectively. At any point along the span, b, the chord is given by

$$c(\bar{y}) = \bar{X}_{T.E.}(\bar{y}) - \bar{X}_{L.E.}(\bar{y}) \tag{2.20}$$

The planform described in Eq. (2.19) can be transformed into a rectangular one by the transformation,

$$\begin{aligned} \bar{\xi} &= \frac{\bar{x} - \bar{X}_{L.E.}}{\bar{X}_{T.E.} - \bar{X}_{L.E.}} \\ \bar{\eta} &= 2\bar{y}/b \end{aligned} \tag{2.21}$$

For all the cases considered, the wing is symmetric so that

$$\bar{z} = \pm h/2 \tag{2.22}$$

where h is the thickness of the wing.

Combining Eqs. (2.21) and (2.22), we can rewrite the wing geometry as

$$\bar{x} = (\bar{x}_{T.E.} - \bar{x}_{L.E.})\bar{\bar{f}} + \bar{x}_{L.E.}$$

$$\bar{y} = b\bar{\eta}/2$$

$$\bar{z} = \pm h/2 \tag{2.23}$$

with

$$0 \leq \bar{\bar{f}} \leq 1$$
$$-1 \leq \bar{\eta} \leq 1 \tag{2.24}$$

When the wing has an angle of attack, α, the position of any point on the surface is changed to (see Fig. 5).

$$\begin{aligned} x &= \bar{x}\cos\alpha + \bar{z}\sin\alpha \\ y &= \bar{y} \\ z &= \bar{z}\cos\alpha - \bar{x}\sin\alpha \end{aligned} \tag{2.25}$$

For small α and small thickness ratio, τ, Eq. (2.25) can be approximated as

$$\begin{aligned} x &= \bar{x} \\ y &= \bar{y} \\ z &= \bar{z} - \bar{x}\alpha \end{aligned} \tag{2.26}$$

The surface of the wing is divided into small quadrilateral elements. The corner coordinates of the wing boxes are stored and used as input for generating the hyperboloidal surface elements.

A further transformation of the wing geometry is necessary, in order to obtain a more accurate evaluation of φ near the leading edge and near the tip of the wing, where φ varies more rapidly than in other areas. The transformation is given by

$$\begin{aligned} \bar{\xi} &= \bar{\psi}^2 \\ \bar{\eta} &= 1 - (1 - \bar{\theta})^2 \end{aligned} \tag{2.27}$$

and it changes the uniform mesh of size

$$\begin{aligned} \Delta\bar{\psi} &= c/NX \\ \Delta\bar{\theta} &= b/2NY \end{aligned} \tag{2.28}$$

(where NX is the number of boxes in the $\bar{\xi}$-direction and NY is the number of boxes in the $\bar{\eta}$-direction along the semispan) into a nonuniform one, as follows:

- along the $\bar{\eta}$-direction, the boxes are larger near the wing root and smaller near the tip;
- along the $\bar{\xi}$-direction, the boxes are smaller near the leading edge and increase in size as we approach the trailing edge.

2.5.2 Thickness distribution

For most cases considered here the thickness is taken to be

$$h = \tau c_{max} \frac{3\sqrt{3}}{2} \xi^{1/2} (1 - \xi)(1 - \eta^2)^{1/2} \tag{2.29}$$

where C_{max} is the maximum chord, τ is the thickness ratio

$$\tau = \frac{h_{max}}{c_{max}} \tag{2.30}$$

where h_{max} is the maximum value of the thickness for a given section. Another wing profile investigated is the circular biconvex one. The planform is described by Eq. (2.26) and the thickness distribution is given by

$$h = 2\left\{\sqrt{\left[\frac{c^2 + h_{max}^2}{4h_{max}}\right]^2 - \left(x - \frac{x_{LE} - x_{TE}}{2}\right)^2} - \frac{c^2 - h_{max}^2}{4h_{max}}\right. \tag{2.31}$$

As before, c represents the chord and h_{max} represents the maximum thickness. The radius of the circular arc is

$$R = \frac{c^2 + h_{max}^2}{4h_{max}} \tag{2.32}$$

Once the wing profile is selected, a variety of wing planforms (rectangular, swept, delta) can be easily generated by simply changing the leading and trailing edge angles of the wing.

2.4.3 Body geometry

For the wing-body configuration, the wing is attached to a body of revolution composed of a forebody of length L_F and radius

$$r = \frac{1}{2} - \frac{1}{8}(x - x_{L.E.})^2 \tag{2.33}$$

a midsection of length L_m and constant radius $r = 1/2$ and an aftbody of length L_A and constant radius $r = 1/2$ (Fig. 6). The surface of the body is also divided in boxes. Care must be taken in matching the coordinates of the wing and the body boxes at the wing root, in order to prevent discontinuities in surface.

SECTION III

THE WAKE

3.1 Dynamics of the Wake

As mentioned in Section I, the surface σ in Eq. 1.1, surrounds the body and the wake. The effect of the wake, disregarded in Section I, yields an additional term in Eq. (1.4), given by[2,5]

$$I_w = \frac{1}{2\pi} \iint_{\sigma} \Delta\varphi \, \bar{n}_u \cdot \bar{\nabla} \frac{1}{r_h} \, d\sigma \tag{3.1}$$

with

$$\Delta\varphi = \varphi_u - \varphi_l \tag{3.2}$$

This represents a distribution of doublets with intensity $\Delta\varphi$. The geometry of the wake is not known. An iterative procedure can be used to solve the problem: consider the surface of the wake divided into small elements. Assume initially that the wake is composed of straight vortex lines (see next subsection): then find the values of φ_i and then evaluate the velocity at the corner of the elements. Find a new location for the corner of the element such that the elements approximate the stream surface emanating from the trailing edge and repeat the procedure mentioned above. However, a simplified treatment of the wake is considered here.

3.2 Simplified Treatment of the Wake

The simplified treatment of the wake used here consists of assuming that the wake is composed of straight vortex-

lines emanating from the trailing edge and parallel to the x-axis (direction of the flow). For this case, the surface of the wake is divided into infinitely long elements, $\hat{\sigma}_\ell$, with two edges parallel to the x-axis. These elements are the continuation of the elements of the wing having an edge in contact with the trailing edge (Fig. 7).

Hence, by assuming that (in view of the Kutta condition that $\partial(\Delta\varphi)/\partial x = 0$ at the trailing edge), the value of $\Delta\varphi_{TE}$ can be approximated by the value at the centroid of the element $\hat{\sigma}_\ell$ the contribution I_w (see Eq. 3.1) is given by

$$\sum \omega_{iK}\, \varphi_K \tag{3.3}$$

with

$$\omega_{iK} = I_w = \pm \frac{1}{2\pi} \iint_{\hat{\sigma}_\ell} \bar{n}_u \cdot \bar{\nabla}\left(\frac{1}{r_h}\right) d\hat{\sigma}_\ell \tag{3.4}$$

for the elements with an edge in contact with the trailing edge, and

$$\omega_{iK} = 0 \tag{3.5}$$

for the others.

In order to evaluate the integral in Eq. (3.4), it is convenient to consider that the element $\hat{\sigma}_\ell$ is the limit of the parallelepipedal element obtained by truncating the element $\hat{\sigma}_\ell$ at the finite distance (Fig. 8). The limit is obtained by letting

$$\bar{P}_1 = \chi\, \bar{u} \quad = \chi\, \bar{i} \tag{3.6}$$

go to infinity; note that $\bar{u} = \bar{i}$ since two edges are parallel to the x-axis. Note that (see Fig. 8)

$$\bar{P}_0 - \bar{P}_1 = \frac{\bar{P}_+ + \bar{P}_-}{2} = \bar{P}_m \qquad \bar{P}_1 = \chi \bar{i} = \bar{a}_1 \tag{3.7}$$

$$\bar{P}_2 = \frac{\bar{P}_+ - \bar{P}_-}{2} = \bar{P}_d = \bar{a}_2 \qquad \bar{P}_3 = 0 \tag{3.8}$$

It is convenient to separate the contribution from the trailing edge ($\bar{f} = -1$) and the edge that goes to infinity ($\bar{f} = 1$):

$$I_w = \mp \frac{s}{2\pi} \left[J_w(1,\eta) - J_w(-1,\eta) \right]_{\eta=-1}^{\eta=1} \tag{3.9}$$

where (note that $\bar{q} = \bar{P}_m + (1+\bar{f})\chi\bar{i} + \eta \bar{P}_d$)

$$s = \text{sign}\left(\bar{q} \cdot \bar{a}_1 \times \bar{a}_2 \right) = \text{sign}\left[\bar{P}_{md} \cdot \bar{i} \times \bar{P}_d \right) \tag{3.10}$$

with

$$\bar{P}_{md} = \bar{P}_m + \eta \bar{P}_d \tag{3.11}$$

while (note that $\bar{q}(\bar{f}=1) = \bar{P}_{md} + 2\chi\bar{i}$)

$$J_w(1,\eta) = \lim_{\chi\to\infty} \tan^{-1}\left(\frac{-(\bar{q}\times\bar{a}_1)\cdot(\bar{q}\times\bar{a}_2)}{|\bar{q}|\,|\bar{q}\cdot\bar{a}_1\times\bar{a}_2|} \right)_{\bar{f}=1}$$

$$= \lim_{\chi\to\infty} \tan^{-1}\left(\frac{-(\bar{q}\times\bar{i})\cdot(\bar{q}\times\bar{P}_d)}{|\bar{q}|\,(\bar{q}\cdot\bar{i}\times\bar{P}_d)} \right)_{\bar{f}=1}$$

$$= \lim_{\chi\to\infty} \tan^{-1} \frac{-\left[(\bar{P}_m + \eta\bar{P}_d)\times\bar{i}\right]\cdot\left[(\bar{P}_m + 2\chi\bar{i})\times\bar{P}_d\right]}{\left[(\bar{P}_m + \eta\bar{P}_d + 2\chi\bar{i})\cdot(\bar{P}_m + \eta\bar{P}_d + 2\chi\bar{i})\right]^{1/2} |\bar{P}_m\cdot\bar{i}\times\bar{P}_d|}$$

$$= \tan^{-1} \frac{-(\bar{P}_{md}\times\bar{i})\cdot(\bar{i}\times\bar{P}_d)}{|\bar{P}_{md}\cdot\bar{i}\times\bar{P}_d|}$$

$$= \tan^{-1} \frac{\bar{P}_{md} \cdot \bar{P}_d - (\bar{P}_{md} \cdot \bar{\imath})(P_d \cdot \bar{\imath})}{|\bar{P}_{md} \cdot \bar{\imath} \times \bar{P}_d|} \qquad (3.12)$$

and similarly (note that $\bar{q}_0(\xi = -1) = \bar{P}_m + \eta \bar{P}_d = \bar{P}_{md}$)

$$J_w(-1,\eta) = \tan^{-1}\left\{ -\frac{(\bar{q} \times \bar{a}_1) \cdot (\bar{q} \times \bar{a}_2)}{|\bar{q}|\,|\bar{q} \cdot \bar{a}_1 \times \bar{a}_2|} \right\}_{\xi = -1}$$

$$= \tan^{-1}\left\{ \frac{(\bar{q} \times \bar{\imath}) \cdot (\bar{q} \times \bar{P}_d)}{|\bar{q}|\,|\bar{q} \cdot \bar{\imath} \times \bar{P}_d|} \right\}_{\xi = -1}$$

$$= \tan^{-1}\left[\frac{-(\bar{P}_{md} \times \bar{\imath}) \cdot (\bar{P}_{md} \times \bar{P}_d)}{|\bar{P}_{md}|\,|\bar{P}_{md} \cdot \bar{\imath} \times \bar{P}_d|} \right]$$

$$= \tan^{-1}\left\{ \frac{-(\bar{P}_{md} \cdot \bar{P}_{md})(\bar{\imath} \cdot \bar{P}_d) - (\bar{P}_{md} \cdot \bar{P}_d)(\bar{P}_{md} \cdot \bar{\imath})}{|\bar{P}_{md}|\,|\bar{P}_{md} \cdot \bar{\imath} \times \bar{P}_d|} \right\} \qquad (3.13)$$

SECTION IV

RESULTS

4.1 Introduction

The formulation outlined in the previous section has been translated into a computer program. In this section, the numerical results obtained for wings and wing-body combination in steady and oscillatory subsonic flow are presented and compared with existing ones.

4.2 Wing Results

Figures 9 and 10 show the general distribution of the potential ϕ and of the lift coefficient C_L for a wing in subsonic flow.

Figures 11a and 12 present a comparison with the experimental and analytical results of Lessing, Troutman and Menees (Ref. 11). The results are for a wing of aspect ratio AR = 3. The wing profile is a biconvex circular arc, 5% thick, with sharp leading and trailing edges. Figure 11a shows the thickness effect (the pressure distribution on the upper and lower surfaces of the wing) for the wing at zero angle of attack and Mach number M = .24. Figure 12 represents the lift distribution for α = 5° and M = .24. The whole wing was divided into 196 elements, or NX = NY = 7 for the upper right hand side of the wing in the X and Y directions, respectively. A convergence study for the problem given for Fig. 11a is presented in Fig. 11b. The curves plotted in Fig. 11b are the distributions of the velocity potential along y = 0 for different numbers of elements. It is shown that the results obtained by using

100 elements on the whole wing, or NX = NY = 5 are accurate enough for general analysis.

Figure 13 shows the lift distribution per unit angle of attack, $C_{\ell\alpha}$, for a rectangular wing with AR = 1 and M = .2. These results, obtained with NX = NY = 7 are compared to the ones of Cunningham and Kulakowski and Haskell (Refs. 12 and 13).

Figure 14 shows the distribution of $C\ell_\alpha$ for a tapered swept wing with aspect ratio AR = 3, taper ratio TR = .5, $\Lambda_{\frac{1}{4}}$ = 45° and M = .8. The results obtained with NX = NY = 7 are compared with the ones of Cunningham (Ref. 12) and Kolbe and Boltz (Ref. 14).

Figure 15 shows the distribution of the section lift coefficient per unit angle of attack, $C_{L\alpha}$, for a rectangular wing with aspect ratio AR = 4 and M = .507. The results, obtained with NX = NY = 7 and then 10, are compared with the ones by Yates (Ref. 16).

4.3 Wing-Body Results

Results for wing-body configurations in steady subsonic flow are compared in Fig. 16a with the results presented by Labrujere, Loeve and Slooff.[17] The results were obtained for M = 0 and a rectangular midpositioned wing with chord c = 1, span b = 6, thickness ratio τ = .9, and α_w = 6°. The body is at zero angle of attack and is composed of a forebody with length L_A = 2 and

$$r = 0.5 - 0.125 \left(x - x_{L.E.}\right)^2 \qquad (5.1)$$

a midsection of length $L_M = 1$ and radius, $r = .5$, and an aft-body of constant radius $r = .5$ and length $L_A = 9$. No wake is used on the body. The number of elements is 200 on the whole configuration (NX = 5, NY = 4 on the wing, NX = 2, NY = 3 on the forebody, NX = 5, NY = 3 on the midsection and NX = NY = 3 on the afftbody). In Fig. 16a, the distribution of the wing section lift coefficient is presented. In Fig. 16b the distribution of the difference of the velocity potentials on the upper and lower surface of the fuselage are shown. These results are related to three circumferential stations as shown in the figures. Results for subsonic oscillatory flow are presented in Figs. 17 and 18 for the same wing considered in Fig. 12, oscillating in bending mode

$$Z = .18043\left|\frac{2y}{b}\right| + 1.70255\left|\frac{2y}{b}\right|^2 - 1.13688\left|\frac{2y}{b}\right|^3 + .25387\left|\frac{2y}{b}\right|^4 \qquad (5.2)$$

with $k = \omega c/2U_\infty = .47$, and $M = .24$ (NX = NY = 7). Figure 17 presents a comparison with the results of Lessing, et al., while in Fig. 18, the results are compared with the ones by Lessing, et al., and Albano and Rodden (Ref. 15).

SECTION V

CONCLUDING REMARKS

A finite-element method for linearized steady and oscillatory subsonic potential aerodynamics around complex configurations has been presented. Numerical results have been obtained for wing-body configurations in steady flows and for finite thickness wings in oscillatory flows. However, the formulation is general can be applied to more complex configurations, although, in this case, the accuracy of the method remains to be assessed. For instance, in the case of wing-tail interaction, the roll-up of the wake might play an important role. A rolled-up wake geometry is being considered for lifting surfaces.

The method is very flexible and simple to use; the use of quadrilateral hyperboloidal elements (which can be used to yield any arbitrary closed surface), defined in terms of their corner points, is one of the original features of the method. Another original feature of the method is the simplicity of the expressions for the coefficients, due to the vector formulation of the problem. The method is also accurate and fast, despite the fact that no effort has been made yet to minimize the computation time: as an example, the computer time for the results for subsonic wing-body configurations (Fig. 6), with 200 surface elements is 775 seconds on the IBM 360/ 50 of Boston University's computing center. The results obtained are in excellent agreement with existing ones.

REFERENCES

1. Morino, L., "Unsteady Compressible Potential Flow Around Lifting Bodies Having Arbitrary Shapes and Motions", Boston University, College of Engineering, Department of Aerospace Engineering, TR-72-01, June 1972.

2. Morino, L., "Unsteady Compressible Potential Flow Around Lifting Bodies: General Theory", AIAA Paper, No. 73-196, January 1973.

3. Kuo, C.C. and Morino, L., "Steady Subsonic Flow Around Finite-Thickness Wings", Boston University, Department of Aerospace Engineering, TR-73-02, February 1973.

4. Morino, L. and Kuo, C.C., "Unsteady Subsonic Flow Around Oscillating Finite-Thickness Wings", Boston University, Department of Aerospace Engineering, TR-73-03, February 1973.

5. Morino, L. and Kuo, C.C., "Unsteady Subsonic Compressible Flow Around Finite-Thickness Wings", AIAA Paper No. 73-313, March 1973.

6. Morino, L., "A Finite Element Formulation for Subsonic Flows Around Complex Configurations", Boston University, College of Engineering, TR-73-05, December 1973.

7. Chen, L.T., Suciu, E.O., and Morino, L., "A Finite Element Method For Potential Aerodynamics Around Complex Configurations", AIAA Paper No. 74-107, presented at the AIAA Aerospace Sciences Meeting, Washington, D.C./January 30-February 1, 1974.

8. Ashley, H., and Landahl, M.T., Aerodynamics of Wings and Bodies, Addison-Wesley, 1965.

9. Mangler, K.W., and Smith, J.H.B., "Behaviour of the Vortex Sheet at the Trailing Edge of a Lifting Wing", The Aeronautical Journal of the Royal Aeronautical Society, Vol. 74, Nov. 1970, pp. 905-908.

10. Lamb, Sir H., Hydrodynamics, 6th Edition, Dover, N.Y., 1945.

11. Lessing, H.C., Troutman, J.C. and Menees, G.P., "Experimental Determination of the Pressure Distribution on a Rectangular Wing Oscillating in the First Bending Mode for Mach Numbers from 0.24 to 1.30", NASA TN D-344, 1960.

12. Cunningham, A.M. Jr., "An Efficient, Steady Subsonic Collocation Method for Solving Lifting-Surface Problems," J. Aircraft, Vol. 8, No. 3, March 1971, pp. 168-176.

13. Kulakowski, L.J. and Haskell, R.N., "Solution of Subsonic Nonplanar Lifting Surface Problems By Means of High-Speed Digital Computers," J. of Aerospace Sci., Vol. 28, Feb. 1961, pp. 103-113.

14. Kolbe, C.D. and Boltz, F.W., "The Forces and Pressure Distribution at Subsonic Speeds on a Planar Wing Having 45° of Sweep Back, an Aspect Ratio of 3, and a Taper Ratio of 0.5", RMA51G31, Oct. 1951, NACA.

15. Albano, E. and Rodden, W.P., "A Doublet-Lattice Method for Calculating Lift Distribution on Oscillating Surfaces in Subsonic Flows," AIAA J., Vol. 7, No. 2, Feb. 1969, pp. 279-285.

16. Yates, E.C., Jr., Private communication, Boston, 1971.

17. Labrujere, T.E., Loeve, W., and J.W. Sloof, "An Approximate Method for the Calculation of the Pressure Distribution of Wing-Body Combinations at Subcritical Speeds", AGARD Specialist Meeting on Aerodynamic Interference", Silver Springs, Md., Sept., 1970, AGARD Conf. Proc. No. 71.

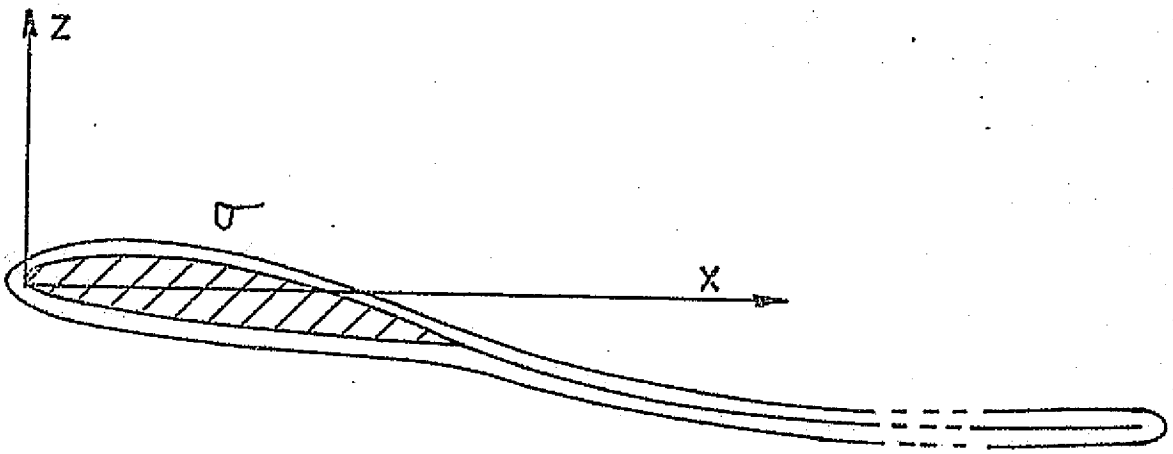

Fig. 1a The surface σ

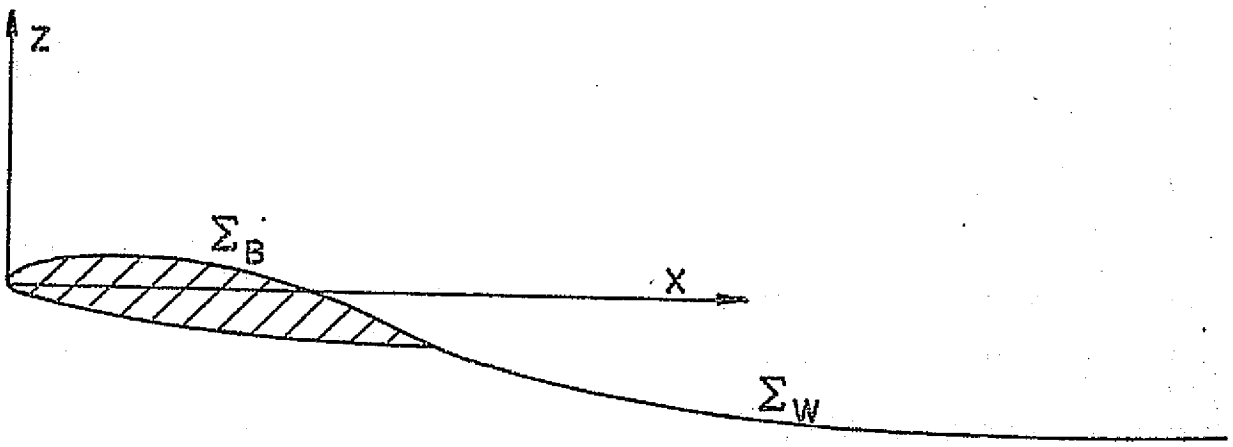

Fig. 1b. The surfaces σ_B and σ_W

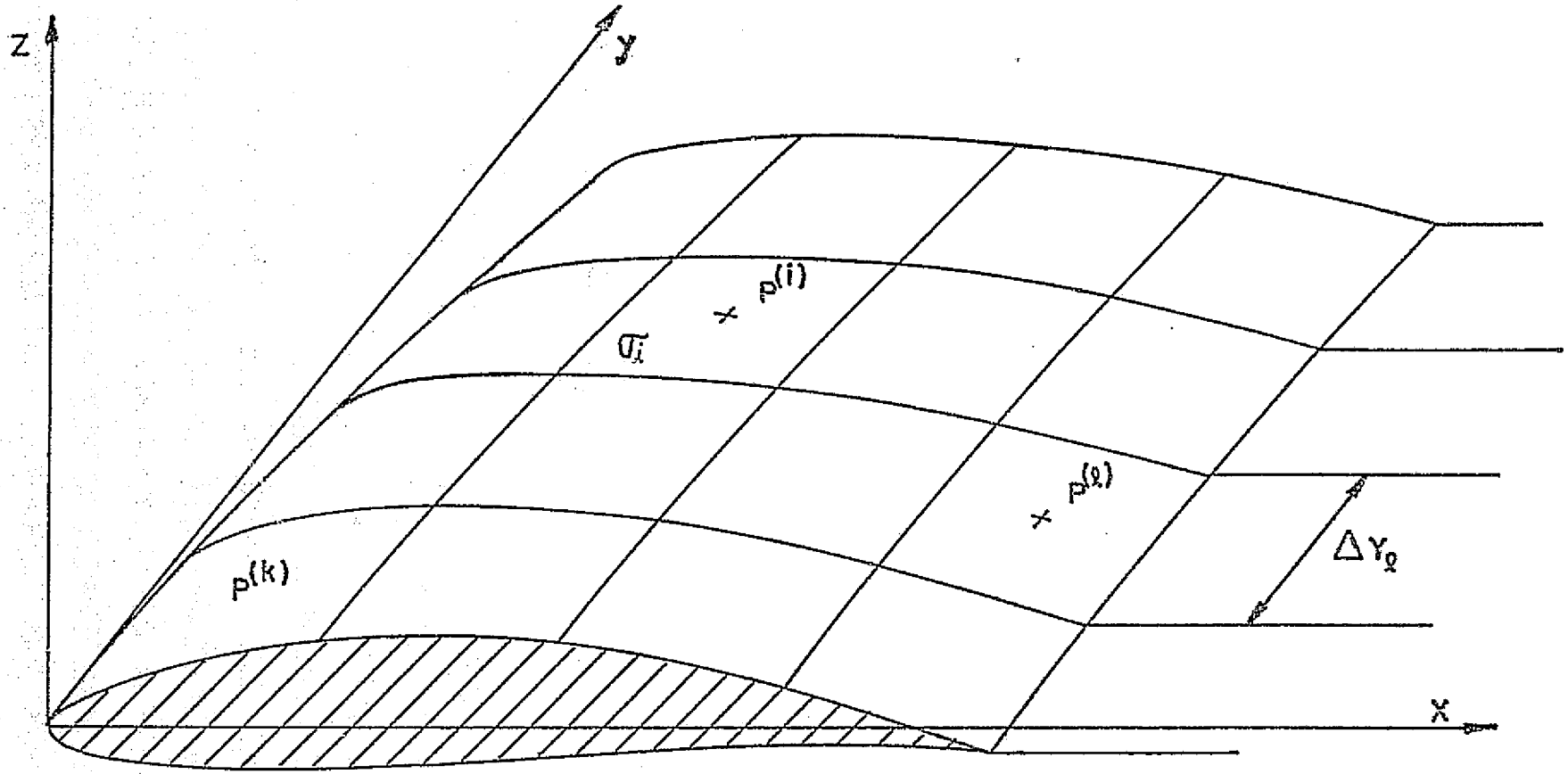

Fig. 2 Boxes and control points

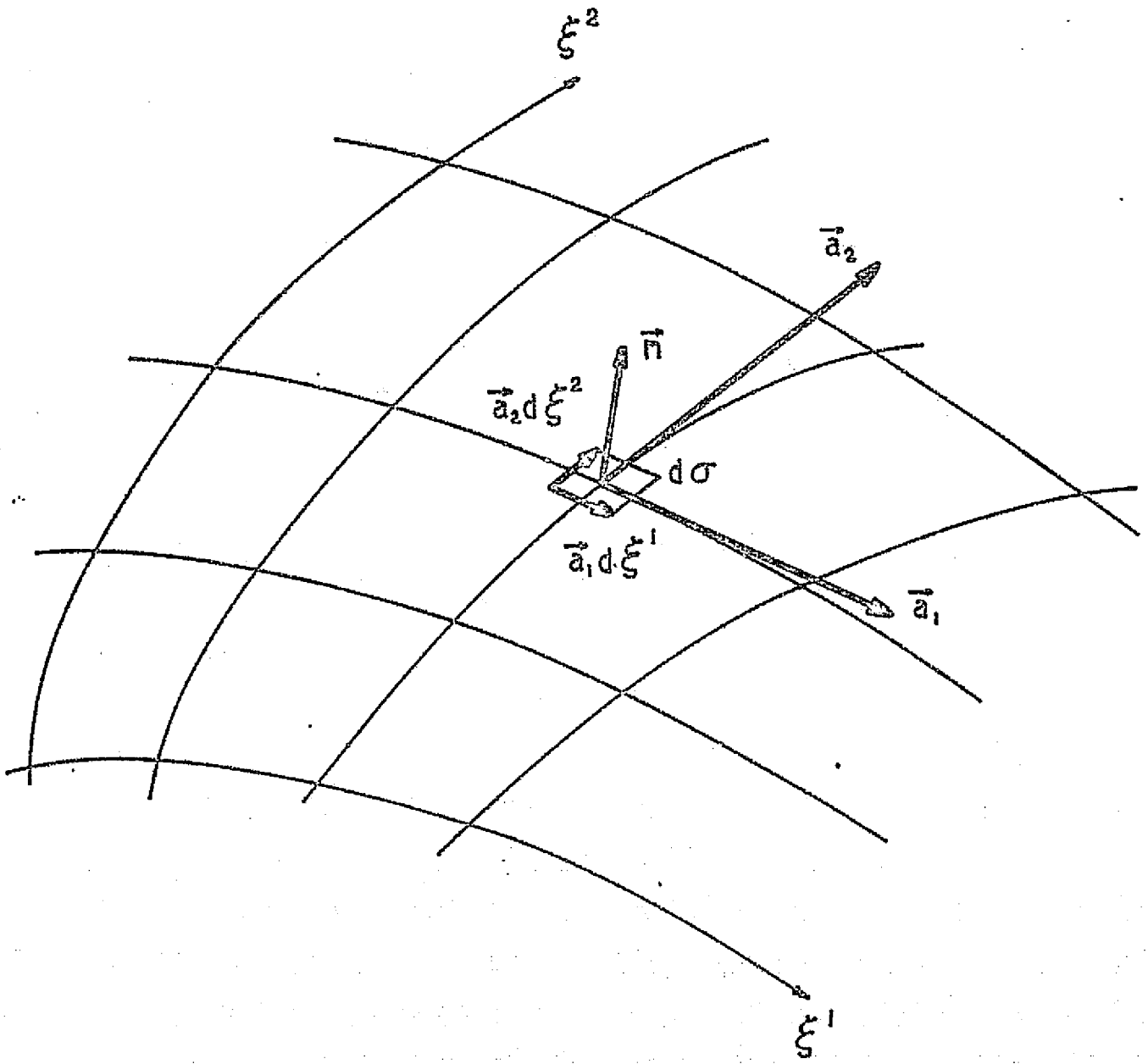

Fig. 3 Surface geometry

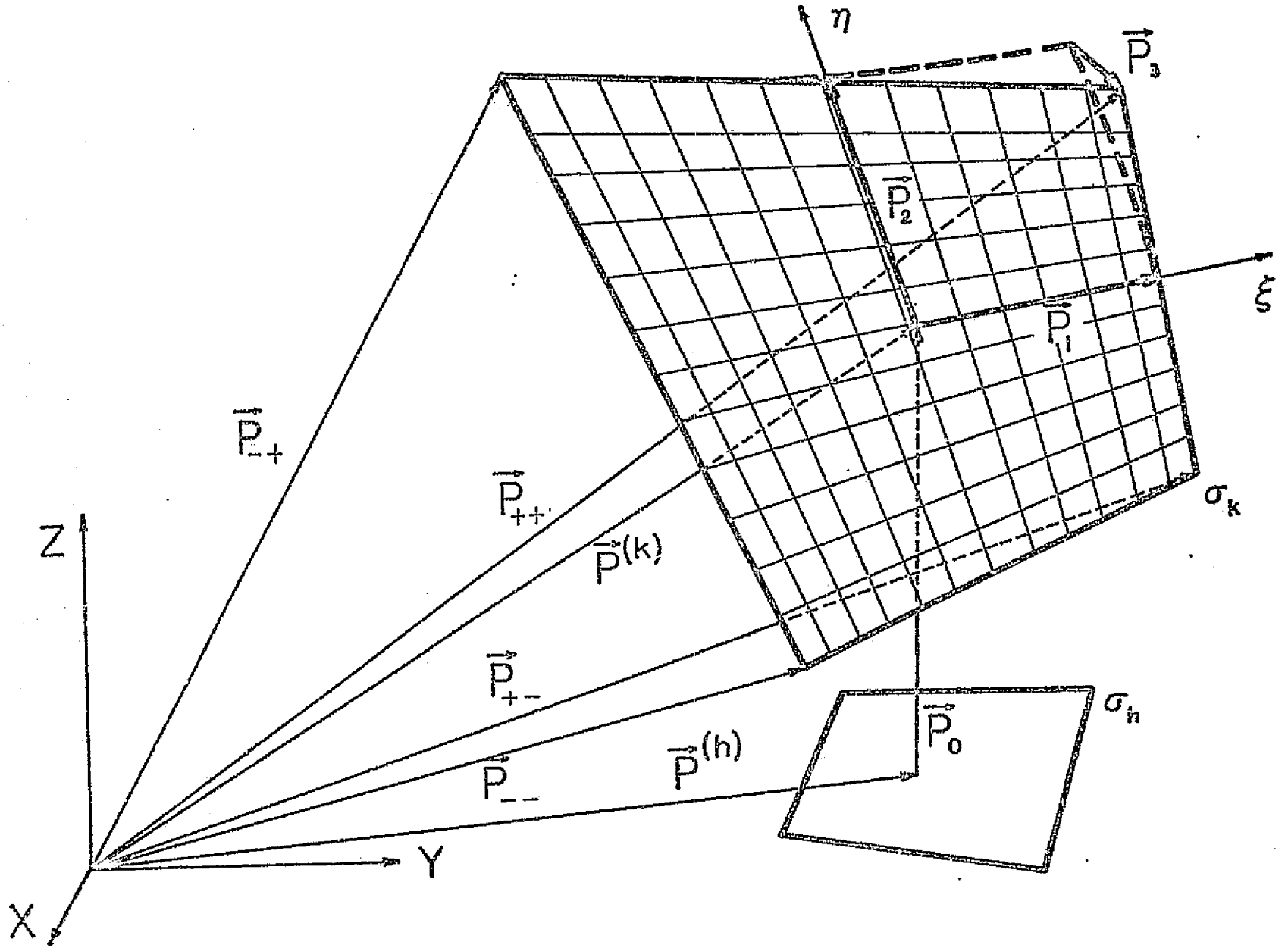

Fig. 4 Geometry of hyperboloidal element

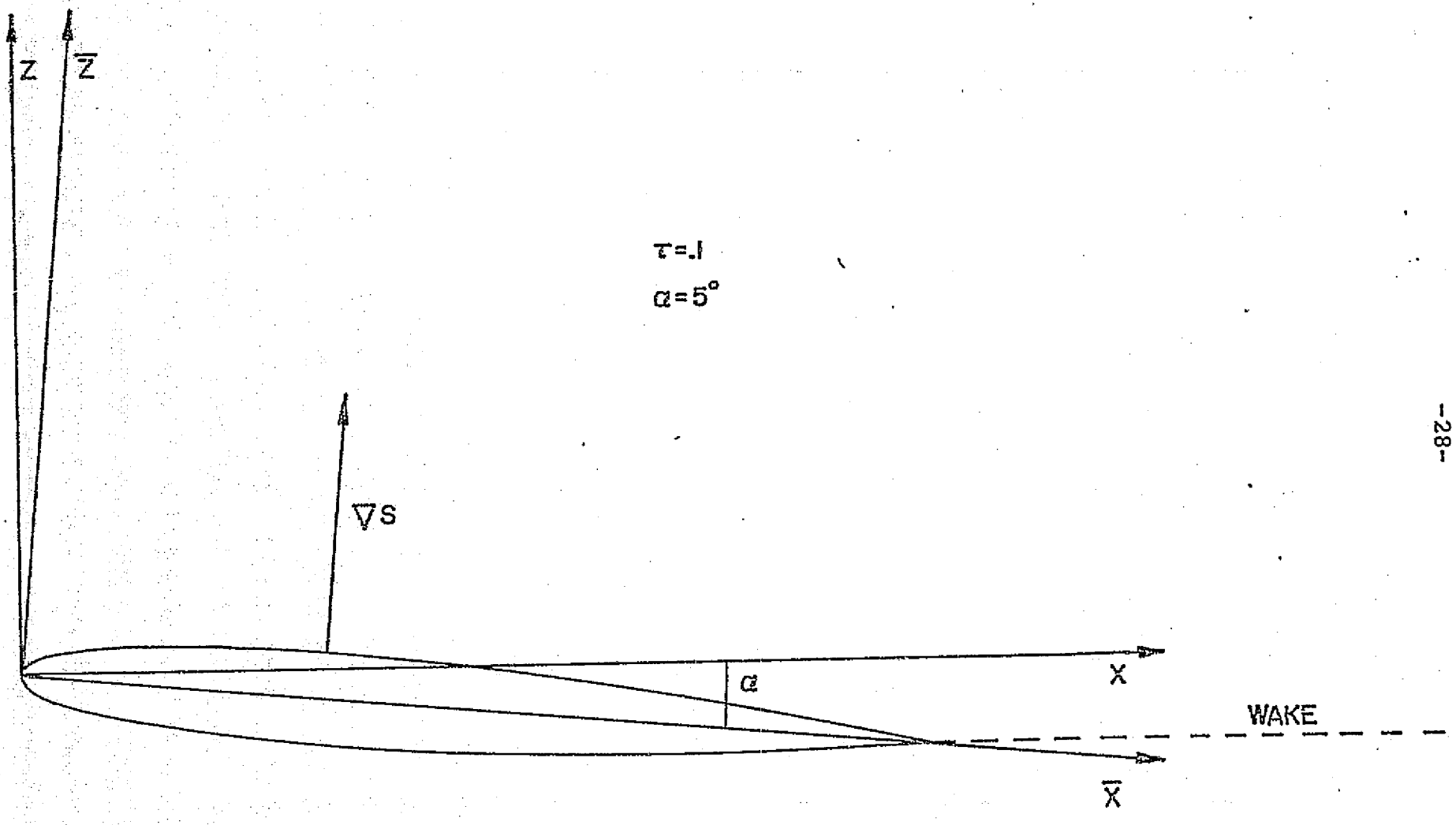

Fig. 5 Geometry of the problem

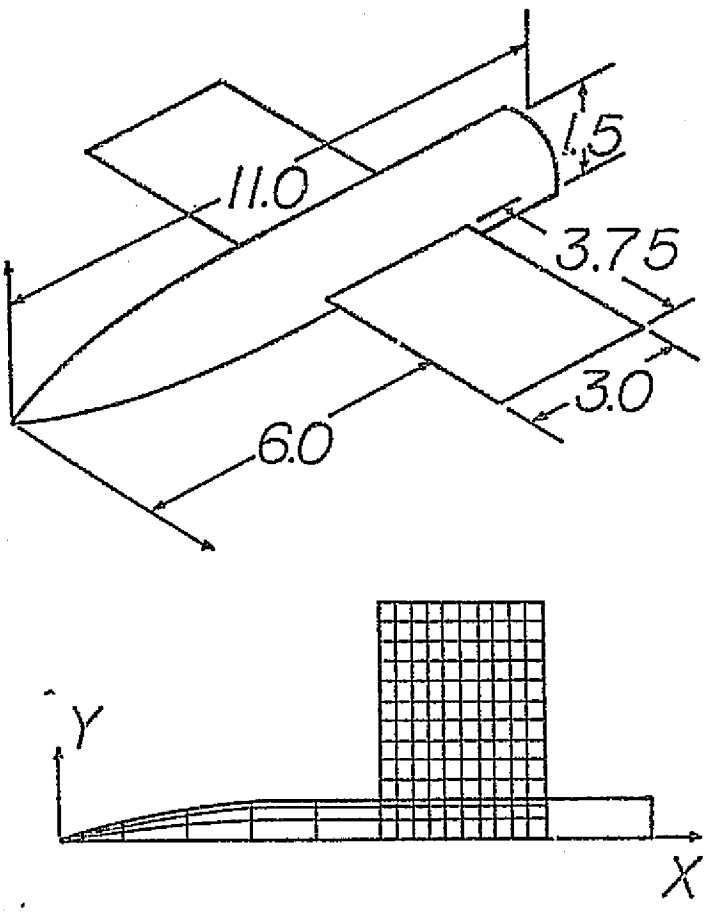

Fig. 6 Wing-Body Configuration

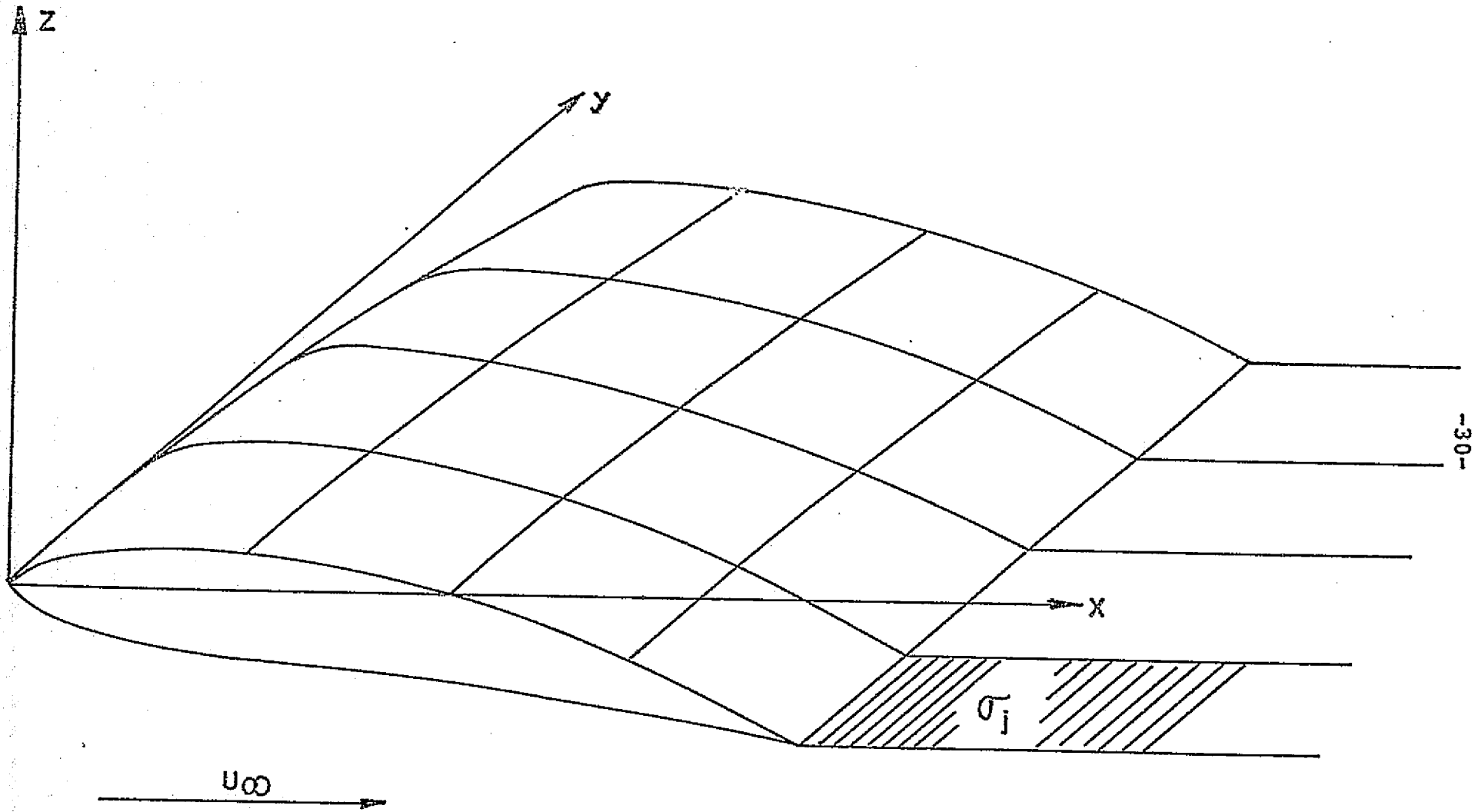

Fig. 7 Treatment of the wake

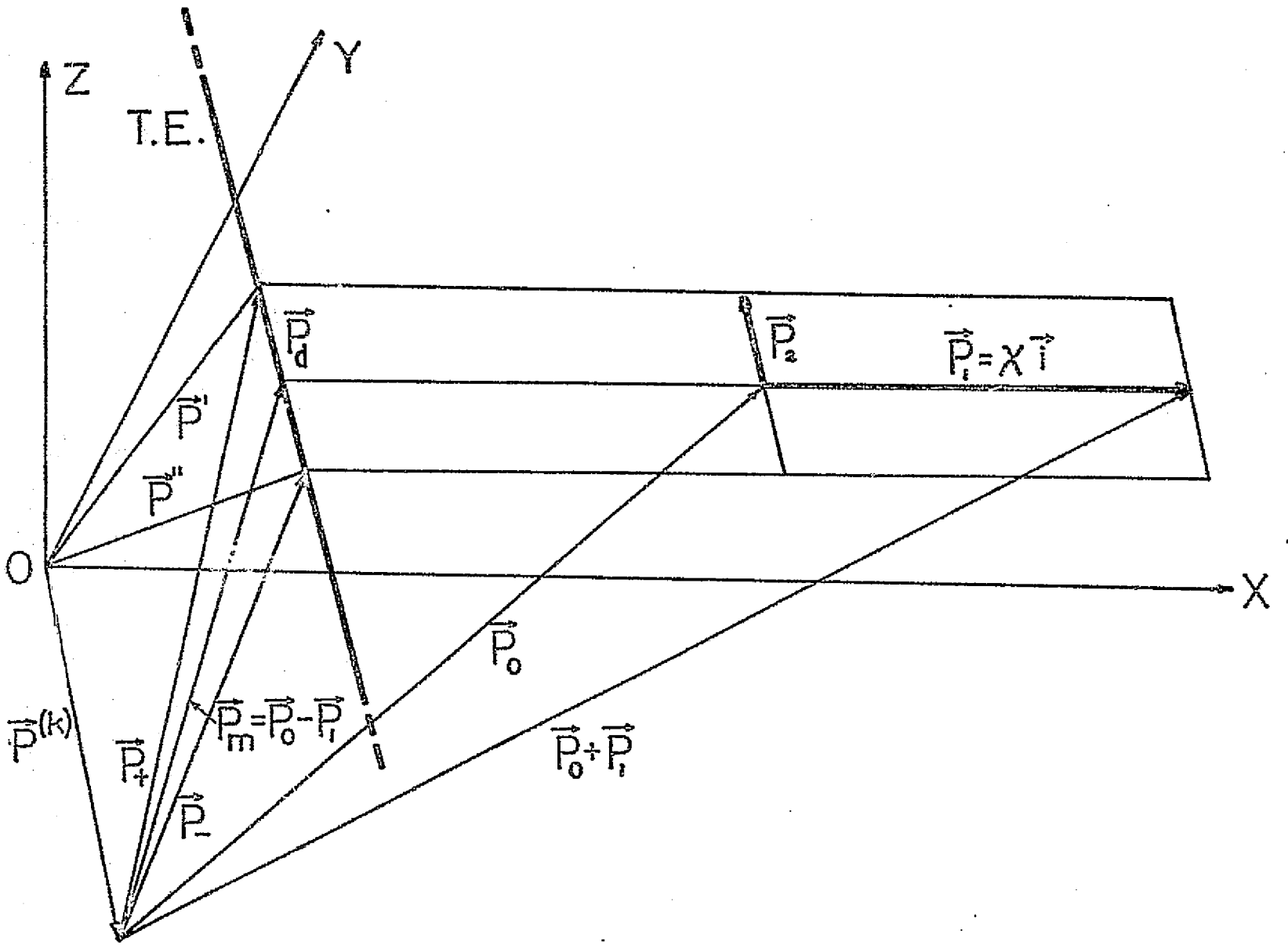

Fig. 8 Wake element

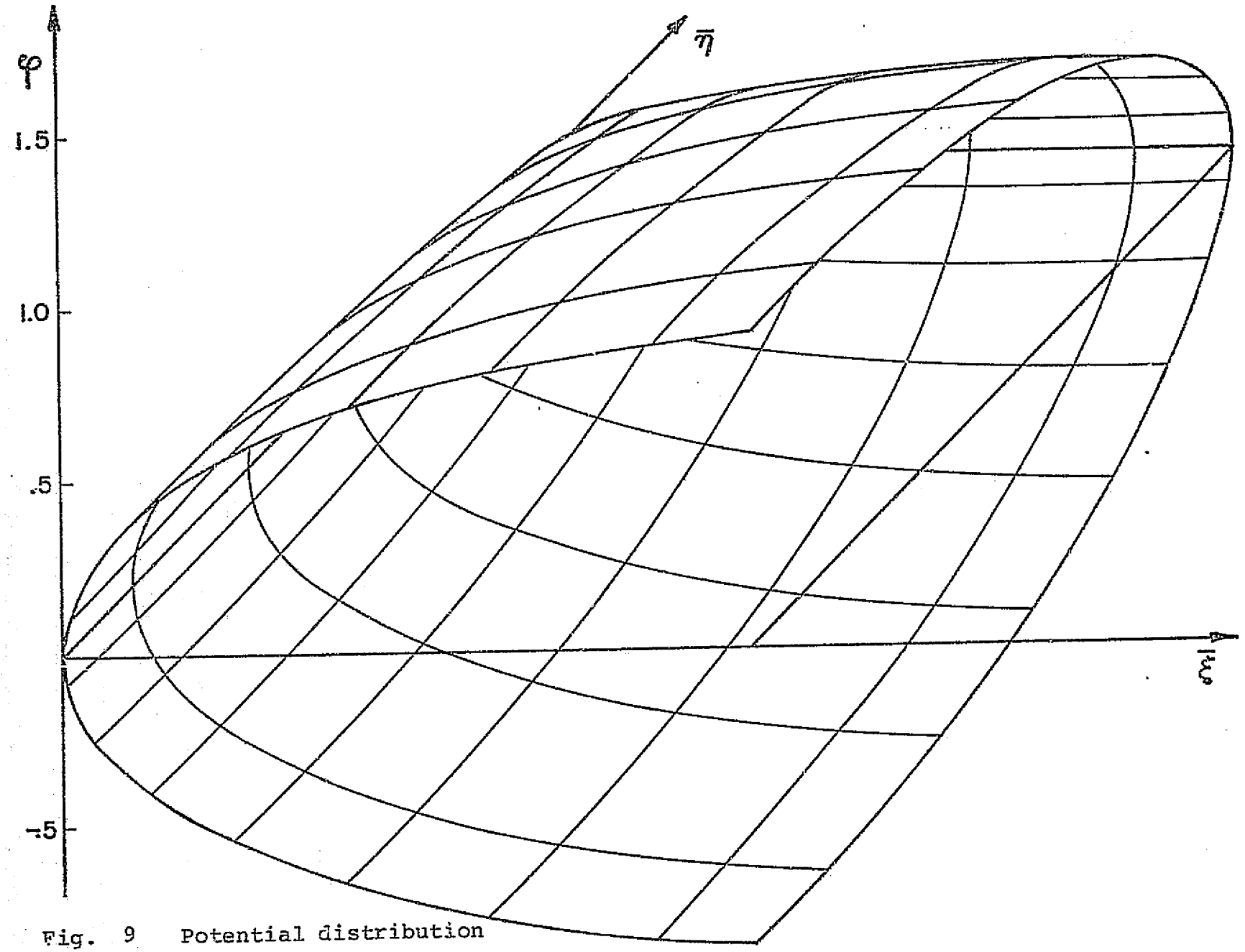

Fig. 9 Potential distribution

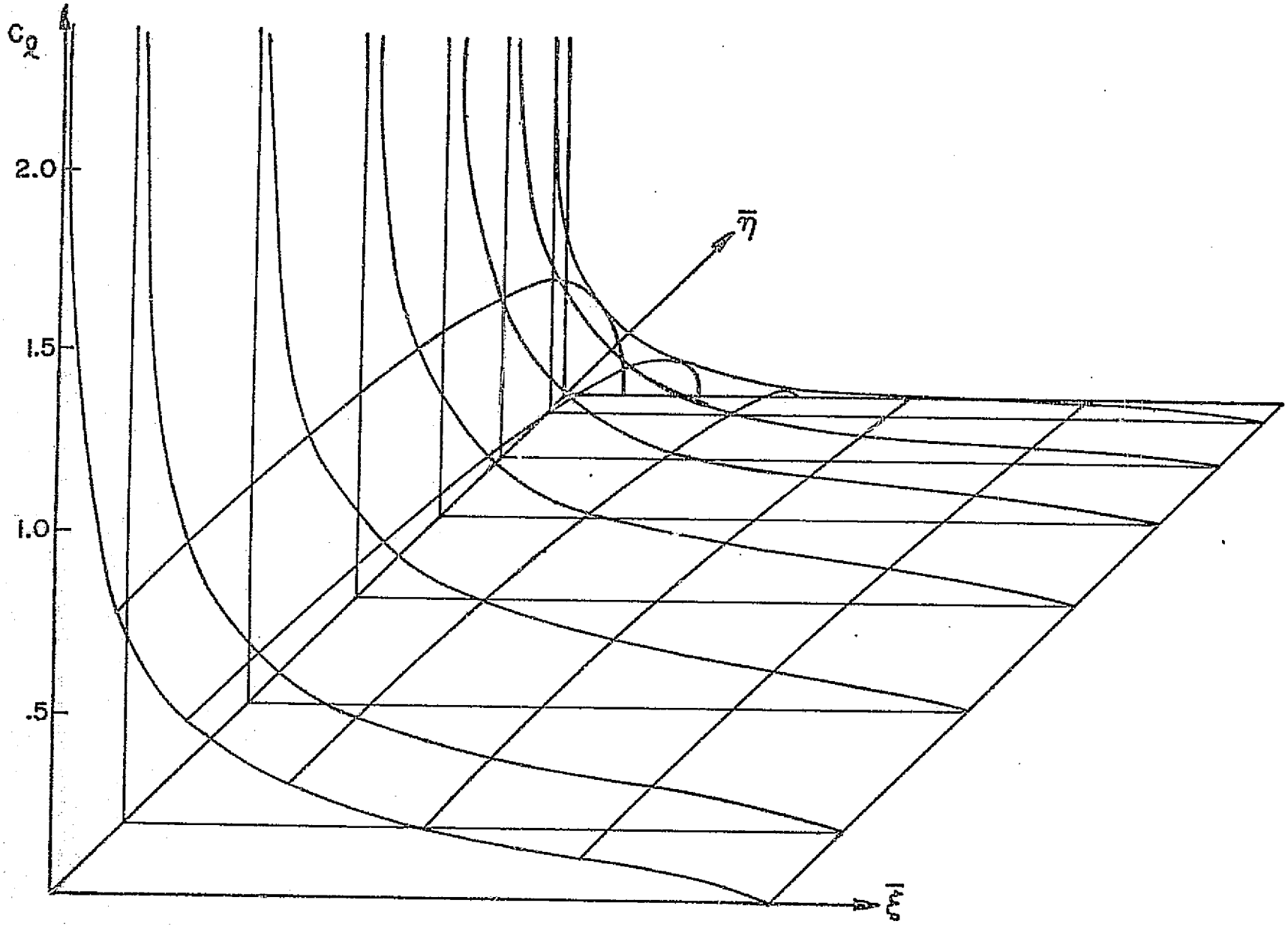

Fig. 10 Lift coefficient distribution

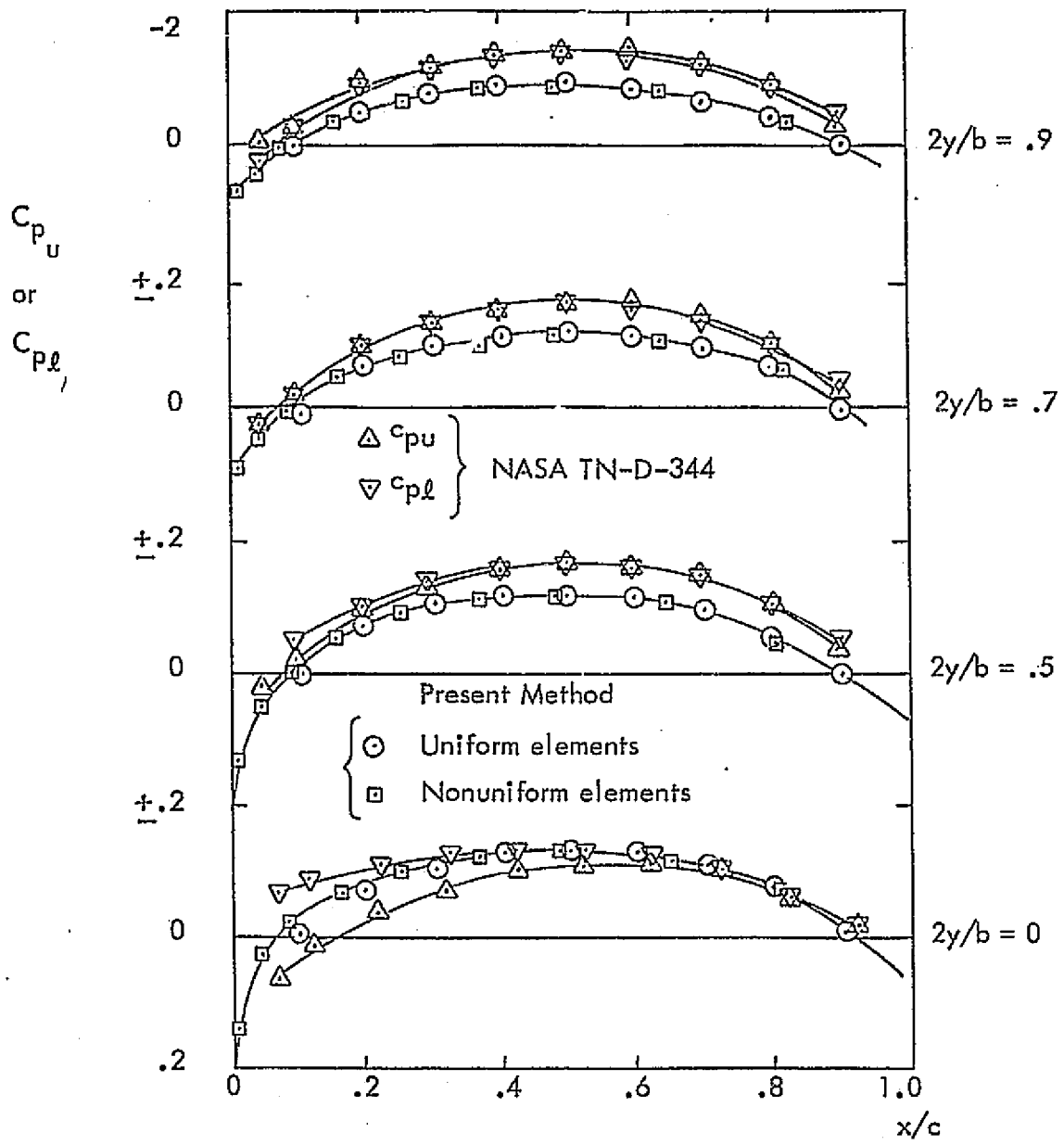

Figure 11a The distribution of c_p on the upper and lower surfaces of a symmetric rectangular wing with AR = 3, τ = 5% α = 0°, M = .24 and NX=NY=10 for comparison with results of Ref. 11

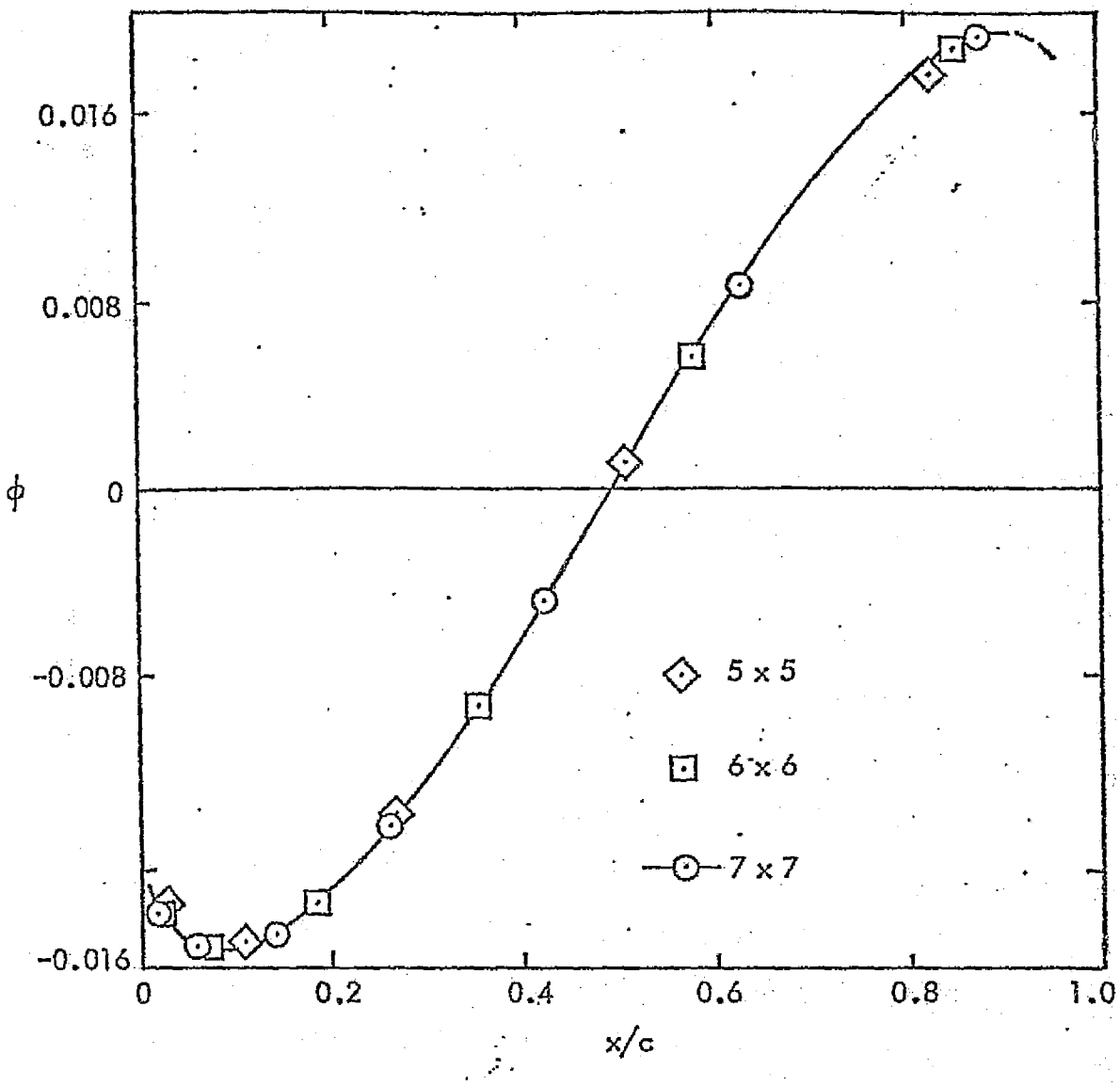

Figure11b Analysis of Convergence: Potential Distribution, ϕ, Versus x/c, at y = 0, for Rectangular Wing With Biconvex Section, in Steady Subsonic Flow, for AR = 3, τ = 0.05, M = 0.24, $\alpha = 0^{\circ}$. NX = NY = 5, 6, 7.

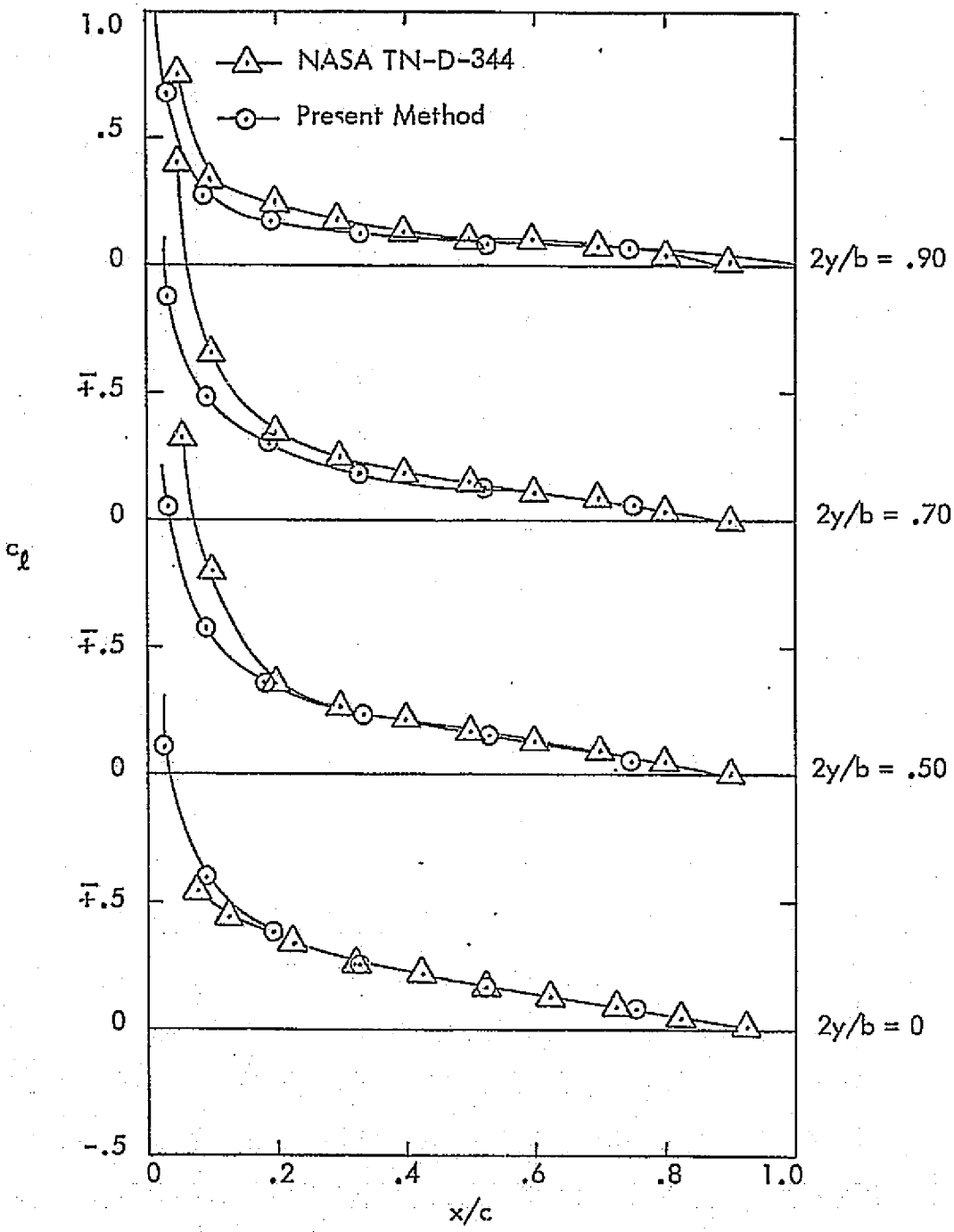

Figure 12 The distribution of the lift coefficient, c_ℓ, on a symmetric rectangular wing with AR = 3, τ = 0.05 α = 5°, M = .24 and NX=NY=7 for comparison with results of Ref. 11

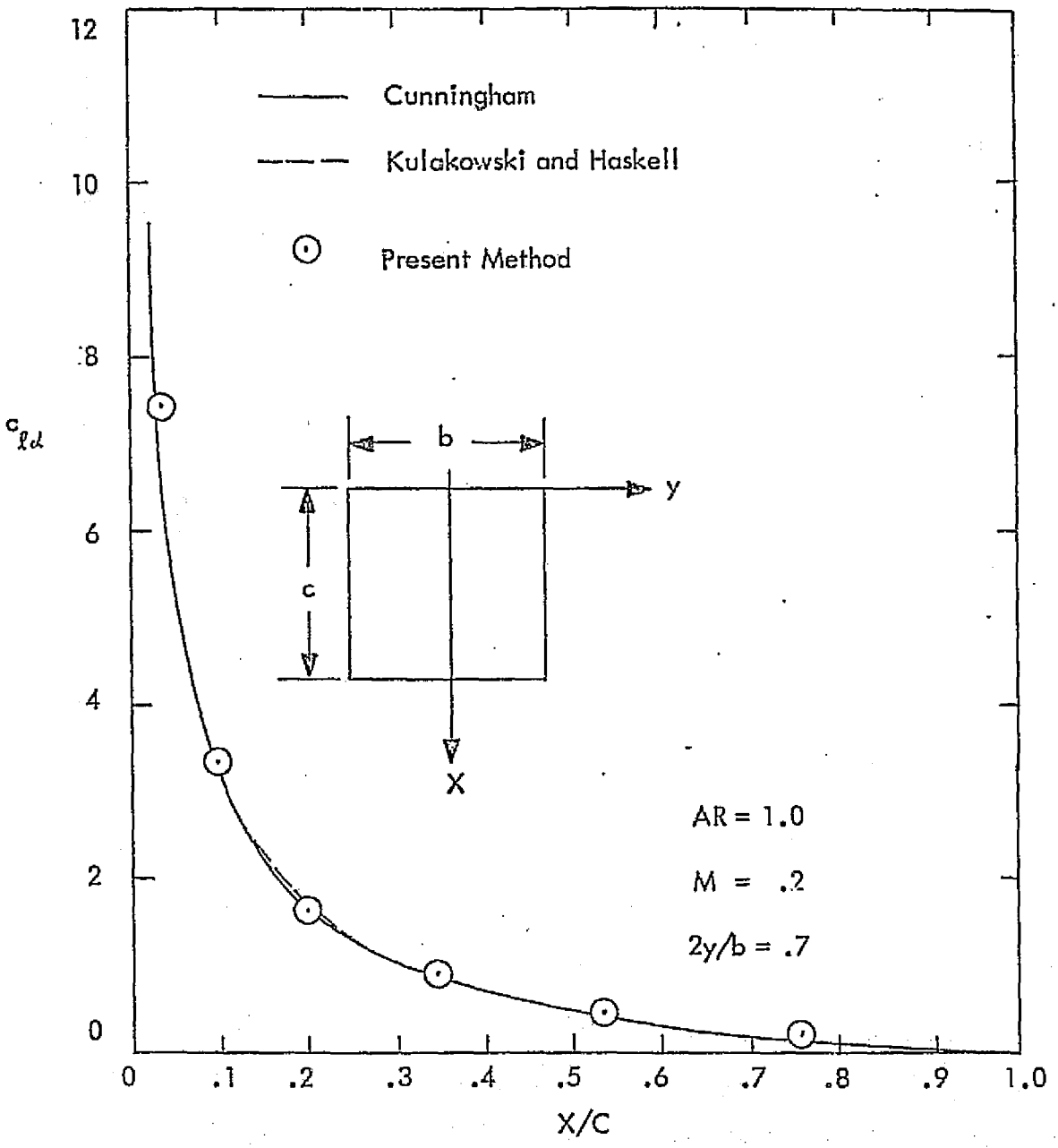

Figure 13 The distribution of $c_{\ell\alpha}$ along 2y/b = .7 for a rectangular wing with AR = 1.0, M = .2, and NX = NY = 7 for comparison with results of Refs. 12 and 13.

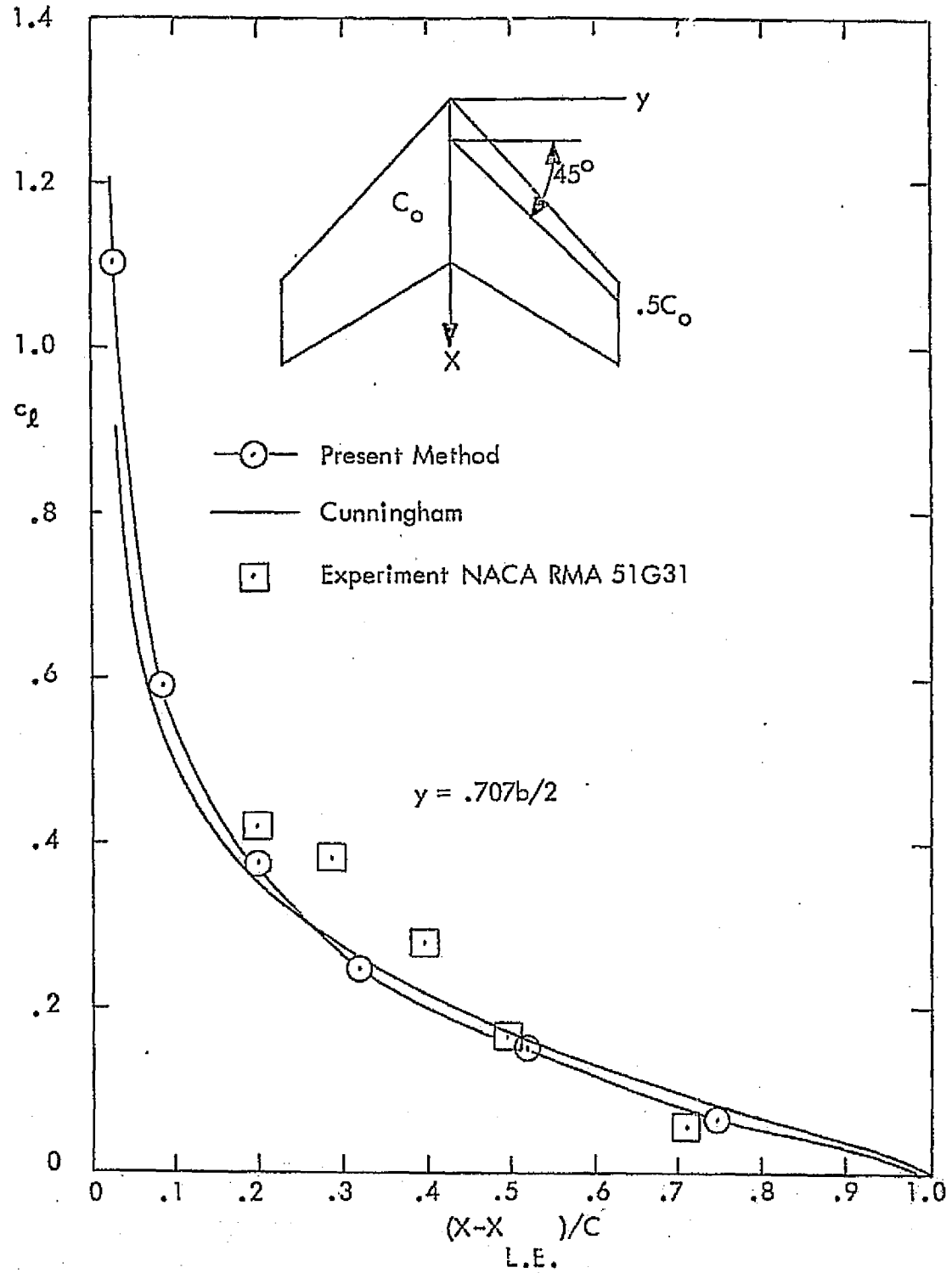

Figure 14 The distribution of c_ℓ along 2y/b = .707 for a tapered swept wing with AR = 3, TR = .5, $\Lambda_{1/4}$ = 45°, M = .8, α = 5° and NX = NY = 7 for comparison with results of Ref. 12 and 14.

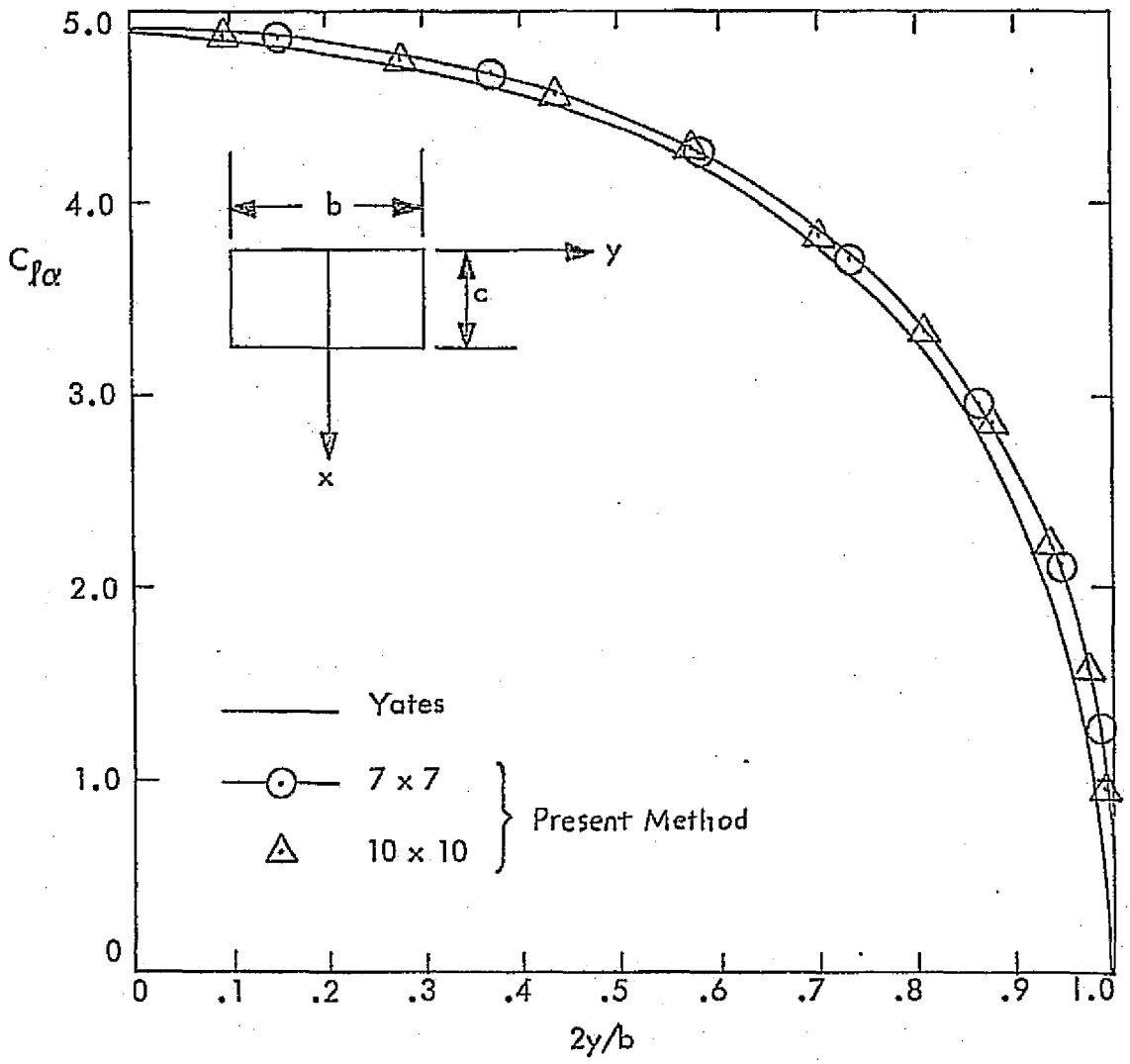

Figure15 The distribution of the section lift coefficient per unit angle of attack for a rectangular wing with AR = 4, M = .507 and NX=NY=7 and 10 for comparison with results of Ref. 16

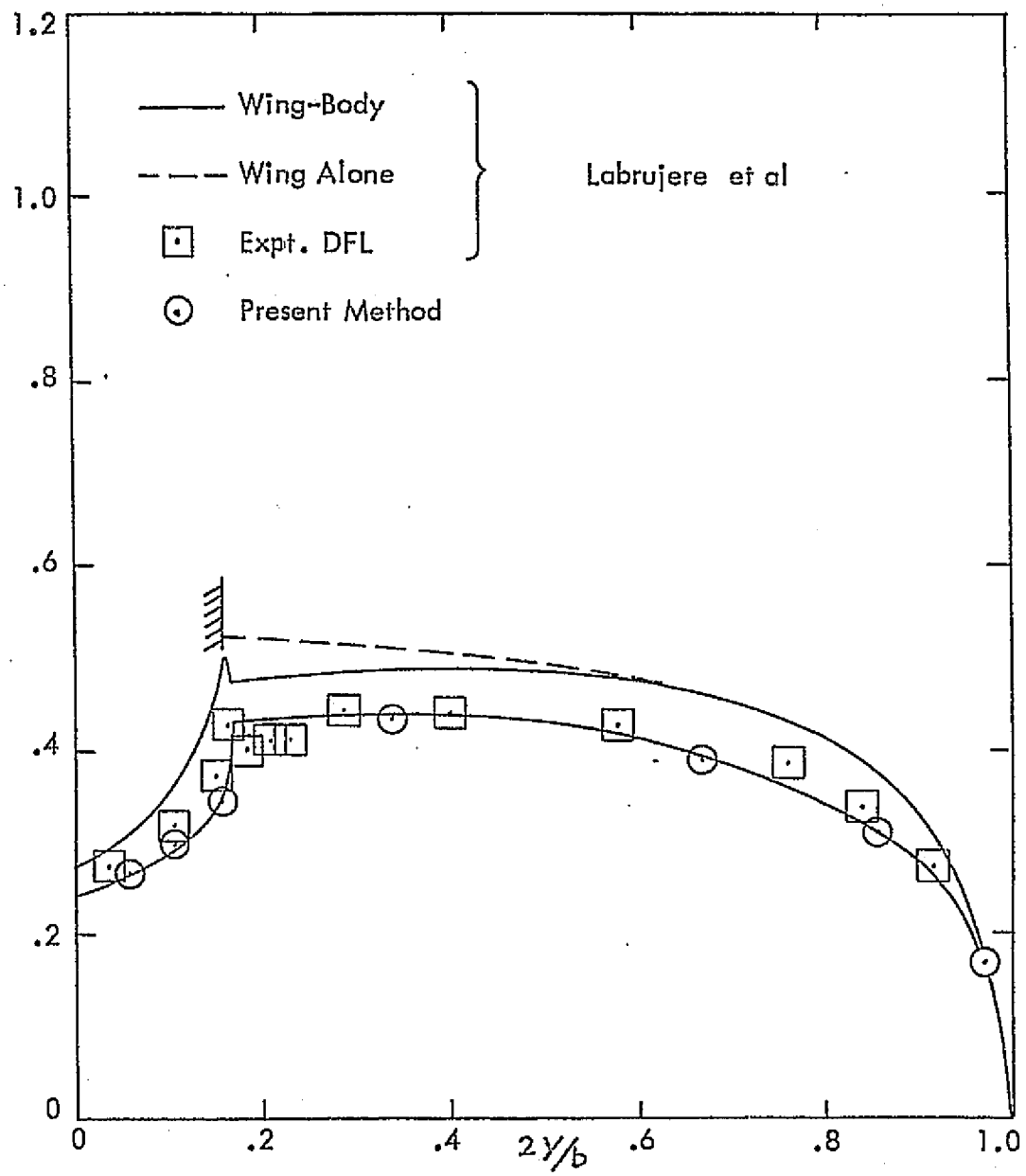

Figure 16a The distribution of section lift coefficient, C_ℓ, for a wing-body configuration with $\alpha_W = 6^o$, $\alpha_B = 0^o$, $\tau = 9\%$, M=0, b=6c, r = 0.5c and 200 elements on the whole wing for the comparison with results of Ref. 17

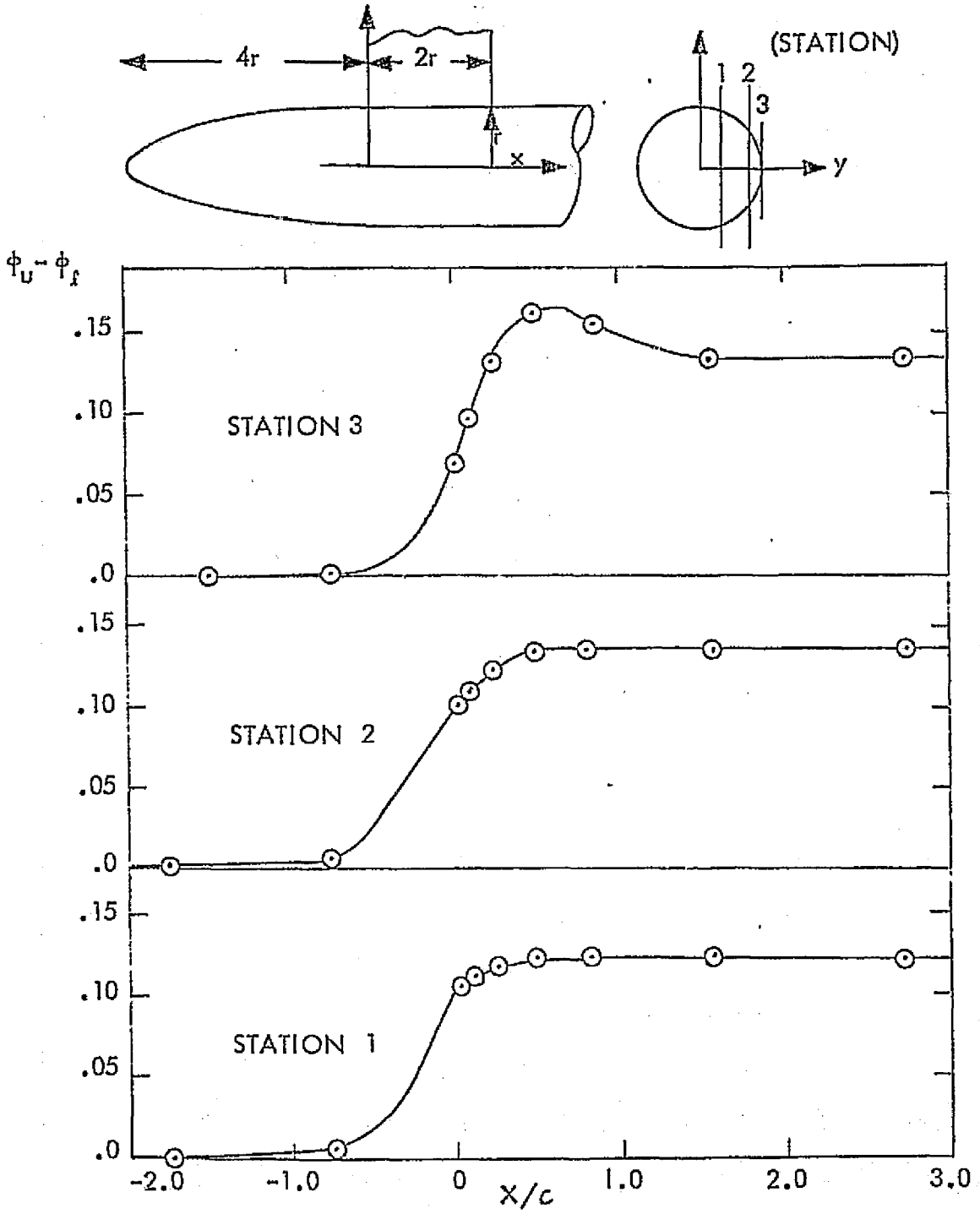

Figure 16b The distribution of $\phi_U - \phi_f$ along three circumferential stations for a wing-body configuration with $\alpha_W = 6^\circ$ $\alpha_B = 0^\circ$, $\tau = 9\%$, M=0, b=6c, r=0.5c

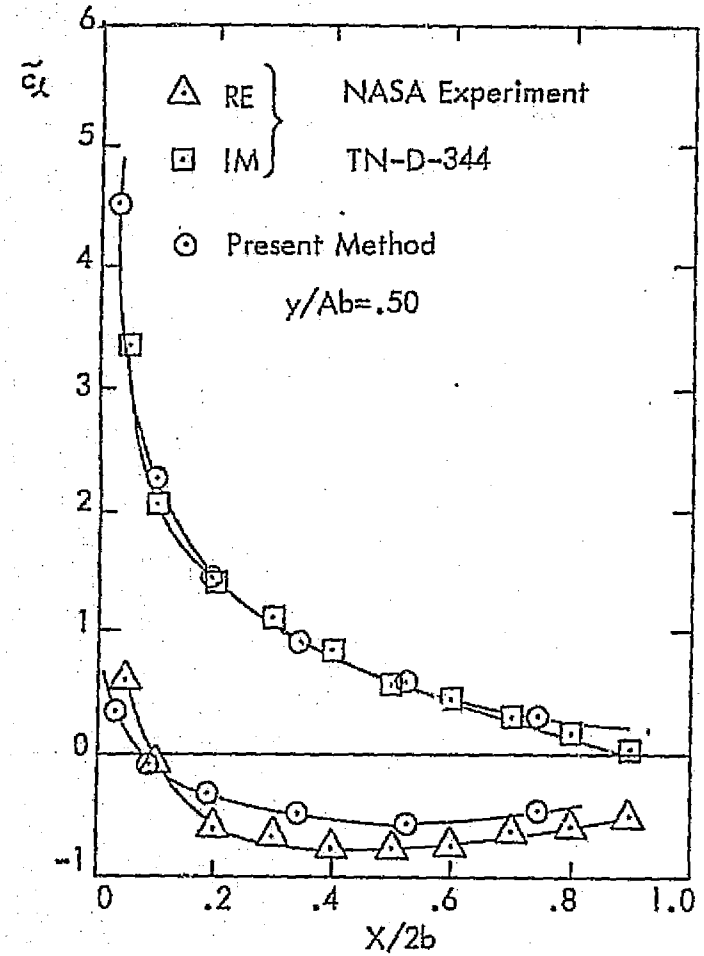

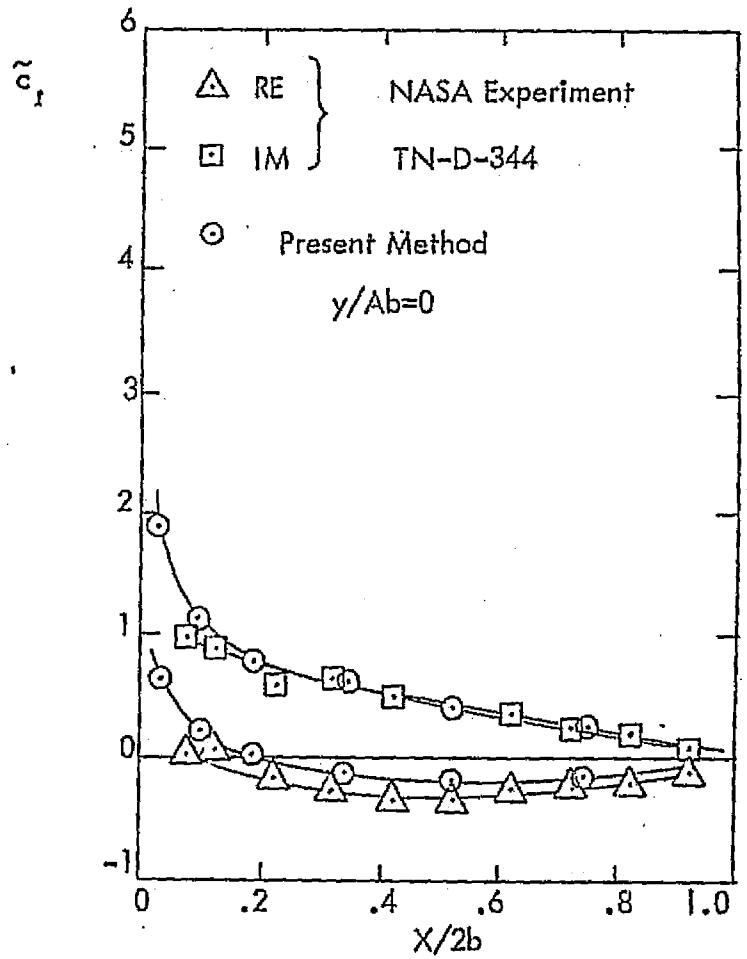

Figure 17 The distribution of lift coefficient, $\tilde{c}_\ell$, for a rectangular wing oscillating in bending mode with $k = \omega c/2U_\infty = .47$, M=.24, AR=3, $\tau = 0.05$, NW =20, L_W=2.5c and NX=NY=7 for comparison with results of Ref. 11

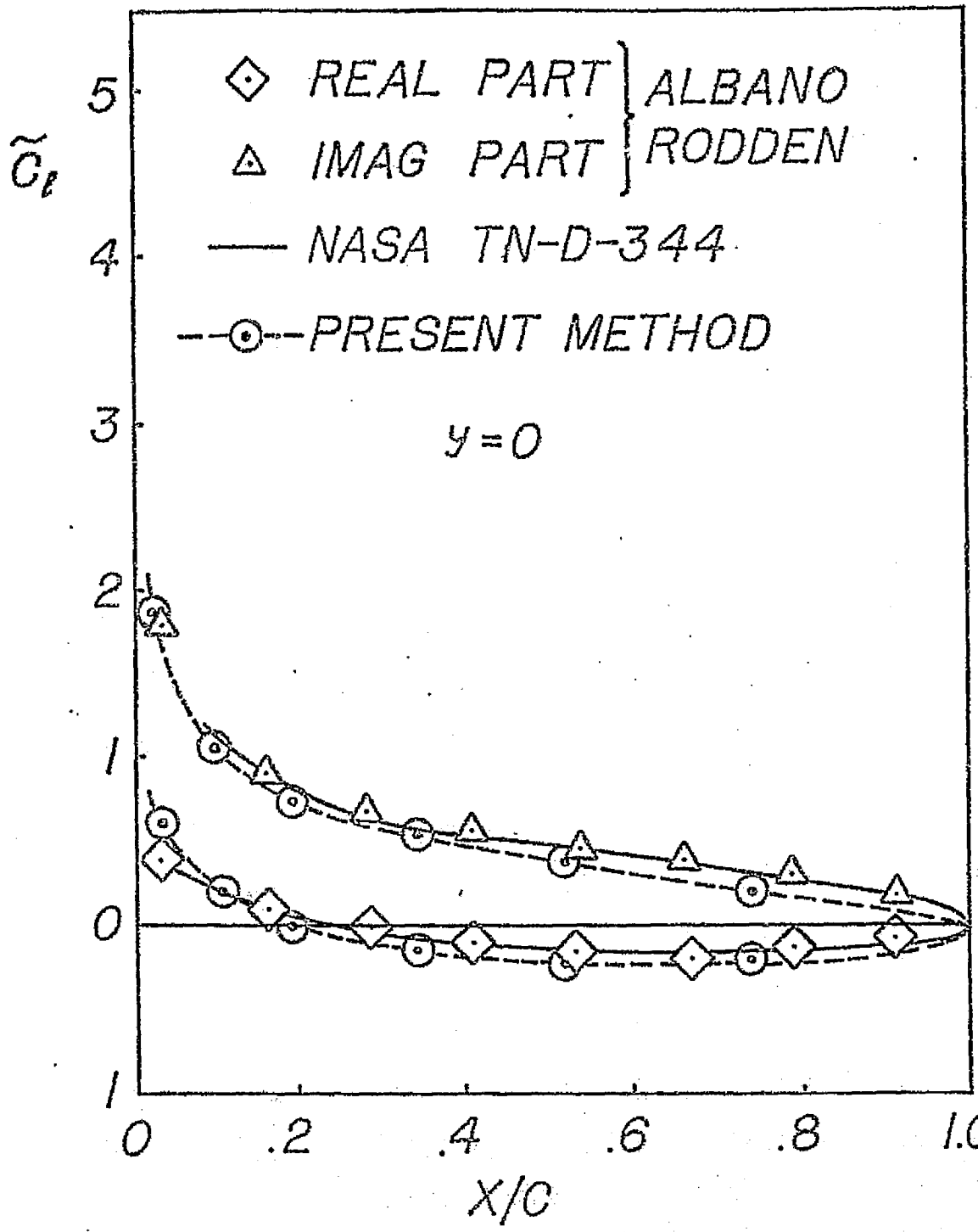

Fig. 18. COMPARISON WITH RESULTS OF REFS. 11 AND 15 FOR RECTANGULAR WING OSCILLATING IN BENDING MODE WITH $k = \omega c/2U_\infty$ = .47, M = .24, AR = 3 and NX = NY = 7.

APPENDIX A

SUBSONIC OSCILLATORY FLOW

A.1 Integral Equation

In this Appendix, it is shown how the results obtained in the main body of this report can be extended to subsonic oscillatory flow. Introducing the variables

$$X = \frac{x}{\beta \ell} \qquad Y = \frac{y}{\ell} \qquad Z = \frac{z}{\ell} \qquad T = \frac{\beta a_\infty t}{\ell} \qquad \Omega = \frac{\omega \ell}{\beta a_\infty} \tag{A.1}$$

and the complex potential $\hat{\phi}$ such that

$$\Phi(x, y, z) = U_\infty \ell \left[X + \hat{\phi}(X, Y, Z) e^{i\Omega(T + MX)} \right] \tag{A.2}$$

the integral equation for the subsonic oscillatory flow is given by

$$2\pi \hat{\phi} = - \iint_\Sigma \left[\frac{\partial \hat{\phi}}{\partial N} \frac{e^{-i\Omega R}}{R} + \hat{\phi} \frac{\partial}{\partial N} \left(\frac{e^{-i\Omega R}}{R} \right) \right] d\Sigma \tag{A.3}$$

where Σ surrounds body and wake.

A.2 Boundary Condition

The boundary condition is given by

$$\nabla_{xyz} S \cdot \nabla_{xyz} \Phi = - \frac{\partial S}{\partial t} - U_\infty \frac{\partial S}{\partial x} \tag{A.4}$$

or

$$\nabla_{XYZ} S \cdot \nabla_{XYZ} \phi + \frac{\beta}{M} \frac{\partial S}{\partial T} + \frac{1}{\beta} \frac{\partial S}{\partial X} + \frac{M^2}{\beta^2} \frac{\partial S}{\partial X} \frac{\partial \phi}{\partial X} = 0 \tag{A.5}$$

where φ and ϕ are such that

$$\Phi = U_\infty x + \varphi = U_\infty \ell (X + \phi) \tag{A.6}$$

Next, assume that the motion of the surface consists of small harmonic oscillations around a rest configuration, that is

$$S = S_0(X, Y, Z) + \tilde{S}(X, Y, Z)\, e^{i\Omega T} \tag{A.7}$$

Then, setting

$$\phi = \phi_0(X, Y, Z) + \tilde{\phi}(X, Y, Z)\, e^{i\Omega T} \tag{A.8}$$

one obtains

$$\begin{aligned} &\nabla_{XYZ} S_0 \cdot \nabla_{XYZ} \phi_0 + \left(\nabla_{XYZ} S_0 \cdot \nabla_{XYZ} \tilde{\phi} + \nabla_{XYZ} \tilde{S} \cdot \nabla_{XYZ} \phi_0 \right) e^{i\Omega T} + \\ &\left(\nabla_{XYZ} \tilde{S} \cdot \nabla_{XYZ} \tilde{\phi} \right) e^{i2\Omega T} + \frac{\beta}{M} i\Omega \tilde{S}\, e^{i\Omega T} + \\ &+ \frac{1}{\beta} \left(\frac{\partial S_0}{\partial X} + \frac{\partial \tilde{S}}{\partial X} e^{i\Omega T} \right) \\ &+ \frac{M^2}{\beta^2} \left[\frac{\partial S_0}{\partial X} \frac{\partial \phi_0}{\partial X} + \left(\frac{\partial S_0}{\partial X} \frac{\partial \tilde{\phi}}{\partial X} + \frac{\partial \tilde{S}}{\partial X} \frac{\partial \phi_0}{\partial X} \right) e^{i\Omega T} + \right. \\ &\left. + \frac{\partial \tilde{S}}{\partial X} \frac{\partial \tilde{\phi}}{\partial X} e^{i2\Omega T} \right] = 0 \end{aligned} \tag{A.9}$$

Assuming

$$S_0 = O(1) \tag{A.10}$$

$$\frac{\partial S_0}{\partial X} = O(\varepsilon) \tag{A.11}$$

with

$$\nabla_{xyz} S_0 = O(1) \tag{A.12}$$

and

$$\tilde{S} = O(\epsilon^2) \tag{A.13}$$

$$\Omega = O(1) \tag{A.14}$$

$$\frac{\partial \tilde{S}}{\partial X} = O(\epsilon^2) \tag{A.15}$$

it is easy to see that

$$\phi_0 = O(\epsilon) \tag{A.16}$$

$$\tilde{\phi} = O(\epsilon^2) \tag{A.17}$$

Neglecting the terms which contain $e^{i2\Omega T}$ (of order ϵ^4) and separating the steady from the oscillatory terms, one obtains

$$\nabla_{xyz} S_0 \cdot \nabla_{xyz} \phi_0 + \frac{1}{\beta} \frac{\partial S_0}{\partial X} + \frac{M^2}{\beta^2} \frac{\partial S_0}{\partial X} \frac{\partial \phi_0}{\partial X} = 0 \tag{A.18}$$

$$\nabla_{xyz} S_0 \cdot \nabla_{xyz} \tilde{\phi} + \nabla_{xyz} \tilde{S} \cdot \nabla_{xyz} \phi_0 + \frac{\beta}{M} i\Omega \tilde{S} + \frac{1}{\beta} \frac{\partial \tilde{S}}{\partial X} + \frac{M^2}{\beta^2} \left(\frac{\partial S_0}{\partial X} \frac{\partial \tilde{\phi}}{\partial X} + \frac{\partial \tilde{S}}{\partial X} \frac{\partial \phi_0}{\partial X} \right) = 0 \tag{A.19}$$

Introducing $\hat{\phi}$ such that

$$\tilde{\phi} = \hat{\phi} e^{i\Omega M X} \tag{A.20}$$

Equation (A.19) reduces to

$$\nabla_{xyz} S_0 \cdot \nabla_{xyz} \hat{\phi} e^{i\Omega M X} + i\Omega M \frac{\partial S_0}{\partial X} \hat{\phi} e^{i\Omega M X} + \nabla_{xyz} \tilde{S} \cdot \nabla_{xyz} \phi_0 + \frac{\beta}{M} i\Omega \tilde{S} + \frac{1}{\beta} \frac{\partial \tilde{S}}{\partial X} + \frac{M^2}{\beta^2} \left[\frac{\partial S_0}{\partial X} \left(\frac{\partial \hat{\phi}}{\partial X} + i\Omega M \hat{\phi} \right) e^{i\Omega M X} + \frac{\partial \tilde{S}}{\partial X} \frac{\partial \phi_0}{\partial X} \right] = 0 \tag{A.21}$$

Finally, neglecting terms of order ε^2 in Eq. (A.18) and terms of order ε^3 in Eq. (A.19), one obtains

$$\nabla_{xyz} S_0 \cdot \nabla_{xyz} \phi_0 = -\frac{1}{\beta} \frac{\partial S_0}{\partial x} \tag{A.22}$$

$$\nabla_{xyz} S_0 \cdot \nabla_{xyz} \hat{\phi} = -\left(i \frac{\beta \Omega}{M} \tilde{S} + \frac{1}{\beta} \frac{\partial \tilde{S}}{\partial x} \right) e^{-i \Omega M x} \tag{A.23}$$

In particular for

$$S = \pm \frac{1}{\ell} \left[z - z_0(x,y) - \tilde{z}(x,y)\, e^{i\omega t} \right]$$

(where the upper[lower] sign holds on the upper [lower] surface), one obtains

$$S_0 = \pm \frac{1}{\ell} \left[z - z_0(x,y) \right] \tag{A.24}$$

$$\tilde{S} = \mp \frac{1}{\ell} \tilde{z}(x,y) \tag{A.25}$$

$$\frac{1}{|\nabla_{xyz} S_0|} = |N_z| = \pm N_z \tag{A.26}$$

and

$$\frac{\partial \hat{\phi}}{\partial N} \equiv \frac{\nabla_{xyz} S_0 \cdot \nabla_{xyz} \hat{\phi}}{|\nabla_{xyz} S_0|} = + N_z \left(i k \frac{\tilde{z}}{\ell} + \frac{\partial \tilde{z}}{\partial x} \right) e^{-i \Omega M x} \tag{A.27}$$

where

$$k = \frac{\beta \Omega}{M} = \frac{\omega \ell}{U_\infty} \tag{A.28}$$

Equation (A.27) gives the value of $\partial \hat{\phi} / \partial N$ to be used in Eq. (A.3).

A.3 Pressure Coefficient

The pressure coefficient is given by the linearized Bernoulli theorem as

$$C_p = -\frac{2}{U_\infty^2}\left(\frac{\partial \varphi}{\partial t} + U_\infty \frac{\partial \varphi}{\partial x}\right)$$

$$= -2\left(\frac{\beta}{M}\frac{\partial \phi}{\partial T} + \frac{1}{\beta}\frac{\partial \phi}{\partial X}\right) \qquad \text{(A.29)}$$

For oscillatory flow, setting

$$\phi = \tilde{\phi} e^{i\Omega T} = \hat{\phi} e^{i\Omega(T + MX)} \qquad \text{(A.30)}$$

$$C_p = \tilde{C}_p e^{i\Omega T} \qquad \text{(A.31)}$$

one obtains

$$\tilde{C}_p = -2\left(\frac{\beta}{M} i\Omega \tilde{\phi} + \frac{1}{\beta}\frac{\partial \tilde{\phi}}{\partial X}\right)$$

$$= -2\left[i\Omega\left(\frac{\beta}{M} + \frac{M}{\beta}\right)\hat{\phi} + \frac{1}{\beta}\frac{\partial \hat{\phi}}{\partial X}\right] e^{i\Omega MX}$$

$$= -\frac{2}{\beta}\left[i\frac{\Omega}{M}\hat{\phi} + \frac{\partial \hat{\phi}}{\partial X}\right] e^{i\Omega MX}$$

$$= -\frac{2}{\beta}\left[e^{-i\Omega X/M}\frac{\partial}{\partial X}\left(\hat{\phi} e^{i\Omega X/M}\right)\right] e^{i\Omega MX}$$

$$= -\frac{2}{\beta} e^{-i\Omega\beta^2 X/M}\frac{\partial}{\partial X}\left(\hat{\phi} e^{i\Omega X/M}\right)$$

$$= -\frac{2}{\beta} e^{-ik\beta X}\frac{\partial}{\partial X}\left(\hat{\phi} e^{ikX/\beta}\right) \qquad \text{(A.32)}$$

APPENDIX B

B.1 Introduction

In this Appendix, it will be shown by diffentiation that the results obtained for the doublet and source integrals are valid for any hyperboloidal element.

B.2 Doublet Integrals

The doublet integral is:

$$I_D = \frac{1}{2\pi} \tan_p^{-1} \frac{-(\bar{q} \times \bar{a}_1)\cdot(\bar{q} \times \bar{a}_2)}{\sqrt{\bar{q}\cdot\bar{q}}\,(\bar{q}\cdot\bar{a}_1 \times \bar{a}_2)} \tag{B.1}$$

From Eq. (1.12), it is apparent that

$$\frac{\partial \bar{q}}{\partial \eta} = \bar{a}_2$$

$$\frac{\partial \bar{a}_1}{\partial \eta} = \bar{P}_3$$

$$\frac{\partial \bar{a}_2}{\partial \eta} = 0 \tag{B.2}$$

We can proceed to differentiate Eq. (B.1) with respect to η :

$$2\pi \frac{\partial I_D}{\partial \eta} = \frac{\partial}{\partial \eta} \tan_p^{-1} \frac{-(\bar{q} \times \bar{a}_1)\cdot(\bar{q} \times \bar{a}_2)}{\sqrt{\bar{q}\cdot\bar{q}}\,(\bar{q}\cdot\bar{a}_1 \times \bar{a}_2)} = \frac{1}{1 + \left[\dfrac{(\bar{q} \times \bar{a}_1)\cdot(\bar{q} \times \bar{a}_2)}{\sqrt{\bar{q}\cdot\bar{q}}\,(\bar{q}\cdot\bar{a}_1 \times \bar{a}_2)}\right]^2}$$

$$\left\{\left[(\bar{a}_2 \times \bar{a}_1)\cdot(\bar{q} \times \bar{a}_2) + (\bar{q} \times \bar{P}_3)\cdot(\bar{q} \times \bar{a}_2) + (\bar{q} \times \bar{a}_1)\cdot(\bar{a}_1 \times \bar{a}_2)\right] \frac{1}{|\bar{q}|\,(\bar{q}\cdot\bar{a}_1 \times \bar{a}_2)}\right.$$

$$\left. + \frac{(\bar{q} \times \bar{a}_1)\cdot(\bar{q} \times \bar{a}_2)}{-(\bar{q}\cdot\bar{q})(\bar{q}\cdot\bar{a}_1 \times \bar{a}_2)}\left[\frac{\bar{a}_2\cdot\bar{q}}{\sqrt{\bar{q}\cdot\bar{q}}}\,\bar{q}\cdot\bar{a}_1 \times \bar{a}_2 + \sqrt{\bar{q}\cdot\bar{q}}\,(\bar{a}_2\cdot\bar{a}_1 \times \bar{a}_2 + \bar{q}\cdot\bar{P}_3 \times \bar{a}_2)\right]\right\}$$

$$= \frac{r^2(\bar{q}\cdot\bar{a}_1\times\bar{a}_2)}{r^2(\bar{q}\cdot\bar{a}_1\times\bar{a}_2)^2+\left[(\bar{q}\times\bar{a}_1)\cdot(\bar{q}\times\bar{a}_2)\right]}\cdot\frac{1}{r^3(\bar{q}\cdot\bar{a}_1\times\bar{a}_2)^2}\times$$

$$\times\left\{\left[(\bar{a}_2\times\bar{a}_1)\cdot(\bar{q}\times\bar{a}_2)+(\bar{q}\times\bar{P}_3)\cdot(\bar{q}\times\bar{a}_2)\right](\bar{q}\cdot\bar{q})(\bar{q}\cdot\bar{a}_1\times\bar{a}_2)\right.$$

$$\left.-(\bar{q}\times\bar{a}_1)(\bar{q}\times\bar{a}_2)\left[(\bar{a}_2\cdot\bar{q})(\bar{q}\cdot\bar{a}_1\times\bar{a}_2)+\bar{q}\cdot\bar{q}(\bar{q}\cdot\bar{P}_3\times\bar{a}_2)\right]\right\}$$

$$= \frac{1}{r^2(\bar{q}\cdot\bar{a}_1\times\bar{a}_2)^2+\left[(\bar{q}\times\bar{a}_1)(\bar{q}\times\bar{a}_2)\right]^2}\cdot\frac{1}{r}$$

$$\times\left\{\left[(\bar{a}_2\times\bar{a}_1)(\bar{q}\times\bar{a}_2)(\bar{q}\cdot\bar{q})-(\bar{q}\times\bar{a}_1)(\bar{q}\times\bar{a}_2)(\bar{a}_2\cdot\bar{q})\right](\bar{q}\cdot\bar{a}_1\times\bar{a}_2)\right.$$

$$\left.+\left[(\bar{q}\times\bar{P}_3)\cdot(\bar{q}\times\bar{a}_2)(\bar{q}\cdot\bar{a}_1\times\bar{a}_2)-(\bar{q}\times\bar{a}_1)(\bar{q}\times\bar{a}_2)(\bar{q}\cdot\bar{a}_1\times\bar{a}_2)\right](\bar{q}\cdot\bar{q})\right\} \tag{B.3}$$

Then, by using the relation

$$\bar{q}\cdot\bar{q}(\bar{q}\cdot\bar{a}_1\times\bar{a}_2)+\left[(\bar{q}\times\bar{a}_1)\cdot(\bar{q}\times\bar{a}_2)\right]^2\equiv|\bar{q}\times\bar{a}_1|^2|\bar{q}\times\bar{a}_2|^2 \tag{B.4}$$

(see Appendix B in Ref. 6) we obtain

$$|\bar{q}\times\bar{a}_1|^2|\bar{q}\times\bar{a}_2|^2-\left\{(\bar{q}\cdot\bar{q})(\bar{q}\cdot\bar{a}_1\times\bar{a}_2)^2+\left[(\bar{q}\times\bar{a}_1)\cdot(\bar{q}\times\bar{a}_2)\right]\right\}^2=0 \tag{B.5}$$

Note that

$$\left[(\bar{a}_2 \times \bar{a}_1)\cdot(\bar{q}\times\bar{a}_2)(\bar{q}\cdot\bar{q}) - (\bar{q}\times\bar{a}_1)\cdot(\bar{q}\times\bar{a}_2)(\bar{a}_2\cdot\bar{q})\right](\bar{q}\cdot\bar{a}_1\times\bar{a}_2)$$

$$+\left[(\bar{q}\times\bar{P}_3)\cdot(\bar{q}\times\bar{a}_2)(\bar{q}\cdot\bar{a}_1\times\bar{a}_2) - (\bar{q}\times\bar{a}_1)\cdot(\bar{q}\times\bar{a}_2)(\bar{q}\cdot\bar{P}_3\times\bar{a}_2)\right](\bar{q}\cdot\bar{q})$$

$$= \left\{\left[(\bar{a}_2\cdot\bar{q})\cancel{(\bar{a}_1\times\bar{a}_2)} - (\bar{a}_2\cdot\bar{a}_2)(\bar{a}_1\cdot\bar{q})\right](\bar{q}\cdot\bar{q})\right.$$

$$\left. - \left[(\bar{q}\cdot\bar{q})\cancel{(\bar{a}_1\cdot\bar{a}_2)} - (\bar{q}\cdot\bar{a}_2)(\bar{q}\cdot\bar{a}_1)\right](\bar{a}_2\cdot\bar{q})\right\}(\bar{q}\cdot\bar{a}_1\times\bar{a}_2)$$

$$+\left\{\left[(\bar{q}\cdot\bar{q})(\bar{P}_3\cdot\bar{a}_2) - (\bar{q}\cdot\bar{a}_2)(\bar{q}\cdot\bar{P}_3)\right](\bar{q}\cdot\bar{a}_1\times\bar{a}_2)\right.$$

$$\left. - \left[(\bar{q}\cdot\bar{q})(\bar{a}_1\cdot\bar{a}_2) - (\bar{q}\cdot\bar{a}_2)(\bar{q}\cdot\bar{a}_1)\right](\bar{q}\cdot\bar{P}_3\times\bar{a}_2)\right\}(\bar{q}\cdot\bar{q})$$

$$= -\left[(\bar{q}\cdot\bar{q})(\bar{a}_2\cdot\bar{a}_2) - (\bar{q}\cdot\bar{a}_2)^2\right](\bar{q}\cdot\bar{a}_1)(\bar{q}\cdot\bar{a}_1\times\bar{a}_2)$$

$$+\left\{(\bar{q}\cdot\bar{q})\left[(\bar{a}_2\cdot\bar{P}_3)(\bar{q}\cdot\bar{a}_1\times\bar{a}_2) - (\bar{a}_1\cdot\bar{a}_2)(\bar{q}\cdot\bar{P}_3\times\bar{a}_2)\right]\right.$$

$$\left. - (\bar{q}\cdot\bar{a}_2)\left[(\bar{q}\cdot\bar{P}_3)(\bar{q}\cdot\bar{a}_1\times\bar{a}_2) - (\bar{q}\cdot\bar{a}_1)(\bar{q}\cdot\bar{P}_3\times\bar{a}_2)\right]\right\}\bar{q}\cdot\bar{q}$$

$$= -|\bar{q}\times\bar{a}_2|^2(\bar{q}\cdot\bar{a}_1)(\bar{q}\cdot\bar{a}_1\times\bar{a}_2)$$

$$+|\bar{q}\times\bar{a}_2|^2(\bar{q}\cdot\bar{q})(\bar{q}\cdot\bar{a}_1\times\bar{P}_3) \qquad \text{(B.6)}$$

If Eqs. (B.1), (B.3), (B.4), (B.5), and (B.6) are combined, we obtain

$$\frac{\partial}{\partial\eta}\tan_p^{-1}\ \frac{-(\bar{q}\times\bar{a}_1)\cdot(\bar{q}\times\bar{a}_2)}{\sqrt{\bar{q}\cdot\bar{q}}\,(\bar{q}\cdot\bar{a}_1\times\bar{a}_2)}$$

$$= \pm \frac{1}{r} \frac{(\bar{q}\cdot\bar{a}_1)(\bar{q}\cdot\bar{a}_1\times\bar{a}_2)-(\bar{q}\cdot\bar{q})(\bar{q}\cdot\bar{a}_1\times\bar{P}_3)}{|\bar{q}\times\bar{a}_1|^2} \qquad (B.7)$$

If we now perform the derivative with respect to ξ, we get

$$2\pi \frac{\partial^2 I_D}{\partial\xi\partial\eta} = \mp \frac{\partial^2}{\partial\xi\partial\eta} \tan_P^{-1} \frac{-(\bar{q}\times\bar{a}_1)\cdot(\bar{q}\times\bar{a}_2)}{\sqrt{\bar{q}\cdot\bar{q}}\,(\bar{q}\cdot\bar{a}_1\times\bar{a}_2)}$$

$$= \frac{\partial}{\partial\xi}\left[\frac{(\bar{q}\cdot\bar{q})(\bar{q}\cdot\bar{a}_1\times\bar{P}_3)-(\bar{q}\cdot\bar{a}_1)(\bar{q}\cdot\bar{a}_1\times\bar{a}_2)}{\sqrt{\bar{q}\cdot\bar{q}}\,|\bar{q}\times\bar{a}_1|^2}\right]$$

$$= \frac{1}{|\bar{q}\times\bar{a}_1|^2}\left\{-\frac{\bar{q}\cdot\bar{a}_1}{(\bar{q}\cdot\bar{q})^{3/2}}\left[(\bar{q}\cdot\bar{q})(\bar{q}\cdot\bar{a}_1\times\bar{P}_3)-(\bar{q}\cdot\bar{a}_1)(\bar{q}\cdot\bar{a}_1\times\bar{a}_2)\right]\right.$$

$$+\frac{1}{\sqrt{\bar{q}\cdot\bar{q}}}\left[2(\bar{a}_1\cdot\bar{q})(\bar{q}\cdot\bar{a}_1\times\bar{P}_3)+(\bar{q}\cdot\bar{q})(a_1\cdot a_1\times\bar{P}_3)\right.$$

$$\left.\left.-(\bar{a}_1\cdot\bar{a}_1)(\bar{q}\cdot\bar{a}_1\times\bar{a}_2)-(\bar{q}\cdot\bar{a}_1)(\bar{a}_1\cdot\bar{a}_1\times\bar{a}_2)-(\bar{q}\cdot\bar{a}_1)(\bar{q}\cdot\bar{a}_1\times\bar{P}_3)\right]\right\}$$

$$= \frac{1}{r^3|\bar{q}\times\bar{a}_1|^2}\left[(\bar{q}\cdot\bar{a}_1)(\bar{q}\cdot\bar{a}_1)-(\bar{q}\cdot\bar{q})(\bar{a}_1\cdot\bar{a}_1)\right](\bar{q}\cdot\bar{a}_1\times\bar{a}_2)$$

$$= -\frac{1}{r^3}\,\bar{q}\cdot\bar{a}_1\times\bar{a}_2 \qquad (B.8)$$

This proves Eq. (2.13)

B.3 Source Integral

Now, we will prove by differentialtion that the result ob-

tained for the source integral is valid for any quadrilateral planar element. In this case, since the normal

$$\bar{n} = \frac{\bar{a}_1 \times \bar{a}_2}{|\bar{a}_1 \times \bar{a}_2|} \tag{B.9}$$

is independent of ξ and η, the source integral given by by Eq. (2.17) reduces to

$$I_S = \frac{1}{2\pi} \left\{ -\bar{q} \times \bar{a}_1 \cdot \bar{n} \frac{1}{|\bar{a}_1|} \ln \left(|\bar{a}_1||\bar{q}| + \bar{q} \cdot \bar{a}_1 \right) + \bar{q} \times \bar{a}_2 \cdot \bar{n} \frac{1}{|\bar{a}_2|} \ln \left(|\bar{a}_1||\bar{q}| + \bar{q} \cdot \bar{a}_2 \right) \right\} - \bar{q} \cdot \bar{n} \, I_D \tag{B.10}$$

where I_D is the doublet integral. Note that

$$\frac{\partial \bar{a}_1}{\partial \xi} = 0$$

$$\frac{\partial}{\partial \xi} \left(\bar{q} \times \bar{a}_1 \cdot \bar{n} \right) = \bar{a}_1 \times \bar{a}_1 \cdot \bar{n} = 0 \tag{B.11}$$

and

$$\frac{\partial}{\partial \xi} \ln \left(|\bar{a}_1||\bar{q}| + \bar{q} \cdot \bar{a}_1 \right)$$

$$= \frac{1}{|\bar{a}_1| + \bar{q} \cdot \bar{a}_1} \left[\frac{\bar{q} \cdot \bar{a}_1}{\sqrt{\bar{q} \cdot \bar{q}}} |\bar{a}_1| + \bar{a}_1 \cdot \bar{a}_1 \right] = \frac{\sqrt{\bar{a}_1 \cdot \bar{a}_1}}{\sqrt{\bar{q} \cdot \bar{q}}} \tag{B.12}$$

Then

$$\frac{\partial^2}{\partial \xi \partial \eta} \left[\bar{q} \times \bar{a}_1 \cdot \bar{n} \frac{1}{|\bar{a}_1|} \ln \left(|\bar{a}_1||\bar{q}| + \bar{q} \cdot \bar{a}_1 \right) \right]$$

$$= \frac{\partial}{\partial \eta} \left(\frac{\bar{q} \times \bar{a}_1 \cdot \bar{n}}{\sqrt{\bar{q} \cdot \bar{q}}} \right) = \frac{\bar{a}_2 \times \bar{a}_1 \cdot \bar{n}}{\sqrt{\bar{q} \cdot \bar{q}}} + \frac{\bar{q} \times \bar{P}_3 \cdot \bar{n}}{\sqrt{\bar{q} \cdot \bar{q}}} - \bar{q} \times \bar{a}_1 \cdot \bar{n} \frac{\bar{q} \cdot \bar{a}_2}{r^3} \tag{B.13}$$

Similarly

$$\frac{\partial^2}{\partial \xi \partial \eta} \left[\bar{q} \times \bar{a}_2 \cdot \bar{n} \frac{1}{|\bar{a}_2|} \ln \left(|\bar{a}_2||\bar{q}| + \bar{q} \cdot \bar{a}_2 \right) \right]$$

$$= \frac{\partial}{\partial \xi} \left(\frac{\bar{q} \times \bar{a}_2 \cdot \bar{n}}{\sqrt{\bar{q} \cdot \bar{q}}} \right) = \frac{\bar{a}_1 \times \bar{a}_2 \cdot \bar{n}}{\sqrt{\bar{q} \cdot \bar{q}}} + \frac{\bar{q} \times \bar{P}_3 \cdot \bar{n}}{\sqrt{\bar{q} \cdot \bar{q}}} - \bar{q} \times \bar{a}_2 \cdot \bar{n} \frac{\bar{q} \cdot \bar{a}_1}{r^3} \tag{B.14}$$

Since

$$\frac{\partial}{\partial \xi}(\bar{q}\cdot\bar{n}) = \bar{a}_1\cdot\bar{n} = 0$$

and

$$\frac{\partial}{\partial \eta}(\bar{q}\cdot\bar{n}) = \bar{a}_2\cdot\bar{n} = 0 \qquad \text{(B.15)}$$

and using Eq. (B.8) we get

$$2\pi\frac{\partial^2}{\partial\xi\partial\eta}\left[(\bar{q}\cdot\bar{n})I_D\right]$$

$$= \bar{q}\cdot\bar{n}\ \frac{\bar{q}\cdot\bar{a}_1\times\bar{a}_2}{r^3} \qquad \text{(B.16)}$$

Now, combining Eqs. (B.10), (B.13), (B.14), and (B.16), yields

$$2\pi\cdot\frac{\partial^2 I_s}{\partial\xi\partial\eta} = \frac{|\bar{a}_1\times\bar{a}_3|}{r} + (\bar{q}\cdot\bar{a}_1\times\bar{n})\frac{\bar{q}\cdot\bar{a}_2}{r^3}$$

$$+\frac{|\bar{a}_1\times\bar{a}_2|}{r} - (\bar{q}\cdot\bar{a}_2\times\bar{n})\frac{\bar{q}\cdot\bar{a}_1}{r^3} - \frac{(\bar{q}\cdot\bar{n})\bar{q}\cdot\bar{a}_1\times\bar{a}_2}{r^3}$$

$$= \frac{|\bar{a}_1\times\bar{a}_2|}{r} + \frac{1}{r^3}\left[(-\bar{q}\times\bar{n}\cdot\bar{a}_1)(\bar{q}\cdot\bar{a}_2)+(\bar{q}\times\bar{n}\cdot\bar{a}_2)(\bar{q}\cdot\bar{a}_1)\right.$$

$$\left.-(\bar{q}\cdot\bar{n})(\bar{q}\cdot\bar{a}_1\times\bar{a}_2)\right]$$

$$= 2\,\frac{|\bar{a}_1\times\bar{a}_2|}{r} + \frac{1}{r^3}\left[-(\bar{q}\times\bar{n})\times\bar{q}\cdot(\bar{a}_1\times\bar{a}_2)-(\bar{q}\cdot\bar{n})(\bar{q}\cdot\bar{a}_1\times a_2)\right]$$

$$= 2\cdot\frac{|\bar{a}_1 \times \bar{a}_2|}{r} + \frac{1}{r^3}\Big[(\bar{q}\cdot\bar{n})(\bar{q}\cdot\bar{a}_1\times\bar{a}_2) - (\bar{q}\cdot\bar{q})(\bar{n}\cdot\bar{a}_1\times\bar{a}_2)$$

$$-(\bar{q}\cdot\bar{n})(\bar{q}\cdot\bar{a}_1\times\bar{a}_2)\Big]$$

$$= 2\frac{|\bar{a}_1\times\bar{a}_2|}{r} - \frac{1}{r}|\quad \bar{a}_1\times\bar{a}_2| = \quad \frac{|\bar{a}_1\times\bar{a}_2|}{r}$$

(B.17)

This proves Eq. (1.15).